

Supporting Information

Reversible Self-Assembled Monolayers (rSAMs):

Adaptable surfaces for enhanced multivalent interactions and ultrasensitive virus detection

Sing Yee Yeung, Annabell Mucha, Ravindra Deshmukh, Malak Boutrus, Thomas Arnebrant
and Börje Sellergren

Contents

1	General Experimental	2
1.1	Reagents	2
1.2	Apparatus and methods	2
1.3	Synthesis of OH-terminated amphiphile 1	3
1.4	Synthesis of α -alkyne sialic acid 13	5
1.5	Synthesis of sialic acid terminated amphiphile 2	8
1.6	Synthesis and sialic acid tether 14 for covalent immobilization	10
1.7	Kinetic interaction analysis	11
1.8	Substrates	12
1.9	Infrared reflection-adsorption spectroscopy (IRAS)	13
1.10	Atomic Force Microscopy	13
1.11	Contact Angle	14
2	Supplementary Tables	15
3	Supplementary Figures	22
4	Supplementary Notes	45
5	Supplementary References	47

1 General Experimental

1.1 Reagents

All solvents were purchased from Acros Organics (Geel, Belgium) unless otherwise stated. Acetonitrile (ACN) was obtained from Merck (Darmstadt, Germany). Ethanol (99.5%) was obtained from CCS Health Care (Borlänge, Sweden). Boric acid, (4-(2-hydroxyethyl)-1-piperazineethanesulfonic acid (HEPES) and NaCl were obtained from VWR Chemicals (Leuven, Belgium). MgSO₄, anhydrous was purchased from JT Baker (Japan). Sialic acid was purchased from Carbosynth (Berkshire, UK). Deionized water was used for chemical reactions. All other reagents were purchased from Sigma Aldrich (Sweden) or Merck (Sweden) and used as supplied unless otherwise stated. Details concerning the synthesis and characterisation of EG2 and EG4-SA terminated amidines 15 and 16 and resulting rSAMs will be published separately.

1.2 Apparatus and methods

Thin layer chromatography (TLC) was carried out using Merck aluminium backed sheets coated with 60F254 silica gel. Visualization of the silica plates was achieved using a UV lamp (max = 254 nm), and/or 5% ethanolic H₂SO₄.

HPLC analysis was carried out on a Waters 2695 Alliance HPLC system equipped with autosampler, inline degasser, Waters 2996 PDA detector and MassLynx 4.0 software, using a Phenomenex Luna C18(2) column (4.6 mm (i.d.) x 150 mm, 5 μm, 110 Å) and a guard column (4.6 x 20 mm) at ambient temperature. The mobile phase, as indicated in the procedure (vide infra), was pumped at a flow rate of 1.0 mL min⁻¹.

Flash column chromatography was carried out using Sigma Aldrich silica gel (Merck grade 9385, 60 Å). Reversed phase column chromatography was performed using an Agilent Bond Elute C18 column. The mobile phase used is as specified in the procedure (vide infra).

Proton and carbon nuclear magnetic resonance spectra were recorded using an Agilent (Varian) Mercury 400 MHz instrument operating at 400 or 101 MHz and evaluated using Mestre Nova software. Chemical shifts (δ) are reported in parts per million (ppm) with respect to tetramethylsilane (TMS) using the manufacturers indirect referencing method. All chemical shifts are quoted on the δ scale in ppm using residual solvent as the internal standard. (^1H NMR: $\text{CDCl}_3 = 7.26$, $\text{CD}_3\text{OD} = 4.87$; $\text{DMSO-d}_6 = 2.50$ and ^{13}C NMR: $\text{CDCl}_3 = 77.0$; $\text{CD}_3\text{OD} = 49.0$; $\text{DMSO-d}_6 = 39.5$). Coupling constants (J) are reported in Hz with the following splitting abbreviations: s = singlet, d = doublet, t = triplet, q = quartet, quin = quintet, and m = multiplet.

Low resolution mass spectra (LRMS) were conducted using a Waters ZQ2000 MS system with 2795 LC and 2996 PDA. High resolution mass spectra (HRMS) were recorded by MALDI-MS analysis performed on a hybrid MALDI LTQ Orbitrap XL (Thermo Fisher Scientific, Germany) instrument. Nominal and exact m/z values are reported in Daltons.

FTIR (ATR) spectra were recorded on a Nicolet 6700 instrument with a SmartITR accessory using 64 scans, a standard KBr beamsplitter, a spectral range of $5000\text{-}400\text{ cm}^{-1}$, and a resolution of 4 cm^{-1} . All spectra were processed and analysed using the OMNIC 8 software.

Elemental analysis of carbon, nitrogen and sulphur contents were determined by analysis at the Department of Organic Chemistry, Johannes Gutenberg Universität Mainz using a Heraeus CHN-rapid analyser (Hanau, Germany).

1.3 Synthesis of OH-terminated amphiphiles

4-(10-Bromo-decyloxy)-benzotrile (5) was synthesized according to a modified literature protocol.¹ 1,10-dibromodecane **3** (25 mL, 111 mmols, 10 eq), 4-cyanophenol **4** (1.31 g, 11 mmol, 1 eq) and anhydrous K_2CO_3 (3.00 g, 22 mmols, 2 eq) in dry acetone (7 mL) was stirred at $80\text{ }^\circ\text{C}$ under N_2 atmosphere for 24 hrs. The resulting slurry was cooled, filtered and washed with acetone. The filtrate was collected and concentrated at $40\text{ }^\circ\text{C}$ *in vacuo*. The crude product was later purified using flash chromatography (hexane to 10% ethylacetate in hexane) to give the nitrile **5** as a white amorphous solid (3.05 g, 81 % yield).

TLC (EtOAc:Hexane, 1:9 v/v): $R_F = 0.49$; $^1\text{H-NMR}$ (500 MHz, CDCl_3) δ 7.60 – 7.52 (m, 2H), 6.96 – 6.88 (m, 2H), 3.99 (t, $J = 6.5$ Hz, 2H), 3.40 (t, $J = 6.8$ Hz, 2H), 1.90 – 1.68 (m, 4H), 1.50 – 1.33 (m, 12H); $^{13}\text{C}\{^1\text{H}\}$ NMR (126 MHz, CDCl_3) δ 162.6, 134.1, 119.4, 115.3, 103.8, 68.5, 34.2, 32.9, 29.5, 29.5, 29.4, 29.1, 28.9, 28.3, 26.0; LRMS (m/z): $[\text{M}]^+$ calcd for $\text{C}_{17}\text{H}_{24}\text{BrNO}$, 338.28; found, 337.82, 339.83.

4-(10-(4-(2-hydroxyethyl)phenoxy)decyloxy)benzotrile (7) was synthesized according to a modified literature protocol.¹ Dry acetone (85 mL) was added to 4-(10-bromodecyloxy)benzotrile 5 (1.70 g, 5.0 mmols, 1 eq), 4-(2-hydroxyethyl)phenol 6 (1.40 g, 10 mmols, 2 eq) and K_2CO_3 , anhydrous (1.40 g, 10 mmols, 2 eq) under N_2 atmosphere at 80°C . After 24 hrs, additional 4-(2-hydroxyethyl)phenol 6 (0.31 g, 2.3 mmols, 0.5 eq) and K_2CO_3 , anhydrous (0.38 g, 2.3 mmols, 0.5 eq) was added and the reaction was left to stir at 80°C for a further 48 hrs. The resulting slurry was cooled, filtered and washed with acetone. The filtrate was collected and concentrated at 40°C *in vacuo*. The crude product was purified using flash chromatography (30% ethyl acetate in hexane to 100% ethyl acetate) to give nitrile 7 as white crystalline solid (~99%, 75% purity) and the sample was used in the next step without further purification. A sample was purified to give the analytical data.

TLC (EtOAc:Hexane, 3:7 v/v): $R_F = 0.23$; $^1\text{H-NMR}$ (400 MHz, CDCl_3) δ 7.56 (d, $J = 8.9$ Hz, 2H), 7.13 (d, $J = 8.6$ Hz, 2H), 6.93 (d, $J = 8.9$ Hz, 2H), 6.84 (d, $J = 8.6$ Hz, 2H), 3.99 (t, $J = 6.5$ Hz, 2H), 3.93 (t, $J = 6.5$ Hz, 2H), 3.82 (t, $J = 6.6$ Hz, 2H), 2.80 (t, $J = 6.5$ Hz, 2H), 1.85 – 1.70 (m, 4H), 1.49 – 1.23 (m, 12H); $^{13}\text{C}\{^1\text{H}\}$ -NMR (101 MHz, CDCl_3) δ 162.57, 157.95, 134.07, 130.34, 130.05, 119.44, 115.29, 114.75, 103.74, 68.52, 68.11, 63.95, 38.40, 29.58, 29.56, 29.47, 29.42, 29.40, 29.09, 26.17, 26.03; analysis (% calcd, % found for $\text{C}_{25}\text{H}_{33}\text{NO}_3$): C (75.91, 75.86), H (8.41, 8.59), N (3.54, 3.40).

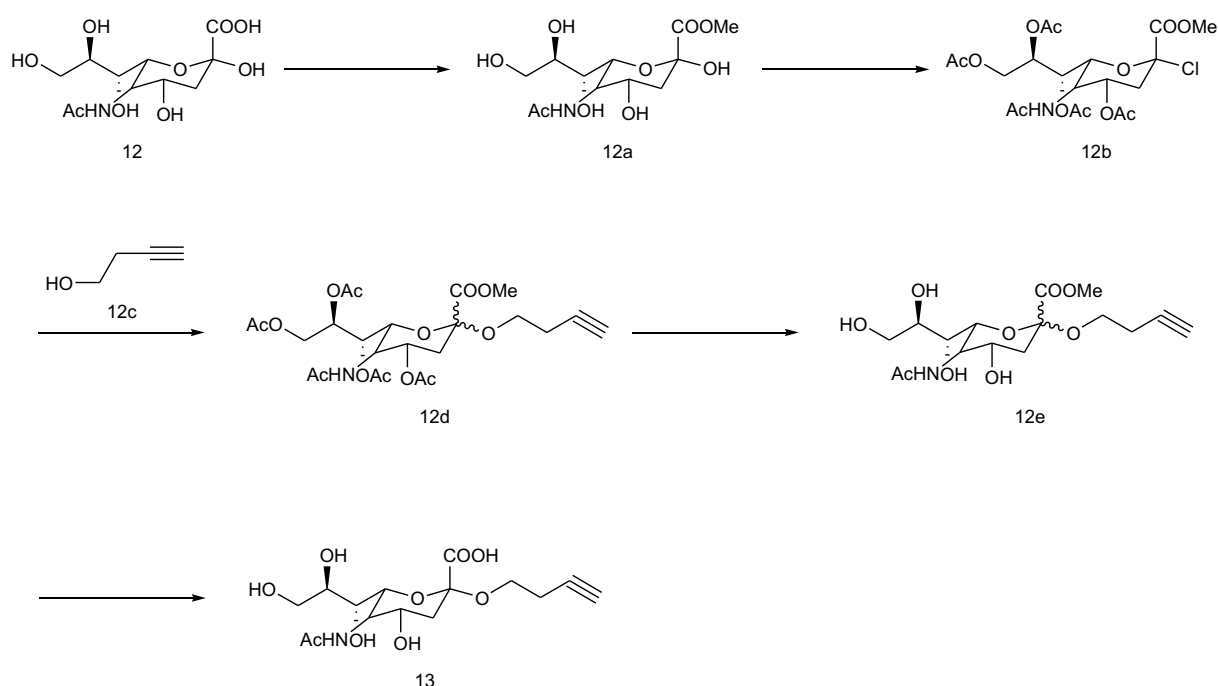
Amino(4-(10-(4-(2-hydroxyethyl)phenoxy)decyloxy)phenyl)methaniminium chloride (1) was synthesized based on a modified literature protocol.² HCl gas was bubbled into a stirred solution 4-(10-(4-(2-hydroxyethyl)phenoxy)decyloxy)benzotrile 7 (1.0 g, 2.5 mmols) in 1,4 dioxane, dry (30 mL) and dry methanol (2.6 mL) at 0°C under N_2 atmosphere. The solution was then left to warm to room temperature and stirred for further 72 hrs. The clear solution was concentrated *in vacuo* at 40°C and the crude imino ester was precipitated in diethyl ether in the freezer overnight. The white precipate was collected via filtration under N_2 atmosphere and reacted with 7M methanolic ammonia (10 mL) and dry methanol (10 mL) at 70°C for 48 hrs. The crude amidine was concentrated *in vacuo* at 40°C , precipitated using diethyl ether

and filtered to give amidine 1 (0.59 g, 53 %) as a white amorphous solid. The product was recrystallized from 2M methanolic HCl prior to characterization and analysis.

m.p.: 206–209 °C; ¹H-NMR (400 MHz, DMSO) δ 9.23 (s, 2H), 9.04 (s, 2H), 7.84 (d, J = 8.8 Hz, 2H), 7.11 (dd, J = 18.6, 8.6 Hz, 4H), 6.80 (d, J = 8.5 Hz, 2H), 4.60 (t, J = 5.2 Hz, 1H), 4.07 (t, J = 6.4 Hz, 2H), 3.90 (t, J = 6.4 Hz, 2H), 3.54 (dt, J = 12.4, 6.3 Hz, 2H), 2.63 (t, J = 7.1 Hz, 2H), 1.78 – 1.62 (m, 4H), 1.47 – 1.22 (m, 12H); ¹³C{¹H}-NMR (101 MHz, DMSO) δ 164.69, 163.07, 156.91, 131.21, 130.14, 129.72, 119.21, 114.73, 114.10, 68.08, 67.28, 62.43, 38.15, 28.91, 28.74, 28.71, 28.44, 25.52, 25.38; analysis (% calcd, % found for C₂₅H₃₇ClN₂O₃): C (66.87, 67.19), H (8.31, 8.41), N (6.24, 6.03).

1.4 Synthesis of α-alkyne sialic acid 13

α-alkyne sialic acid 13 was synthesized based on a modified literature procedure giving an overall yield of 7 % over 5 steps.^{3,4}



Methyl 5-acetamido-2,4-dihydroxy-6-((1R,2R)-1,2,3-trihydroxypropyl)tetrahydro-2H-pyran-2-carboxylate (12a) was synthesized as reported elsewhere.⁴ The ester 12a was isolated as a white amorphous solid (92% yield).

¹H-NMR (400 MHz, CD₃OD) δ 4.03 (m, 2H), 3.87 – 3.79 (m, 3H), 3.78 (d, *J* = 3.7 Hz, 3H), 3.73 – 3.66 (m, 1H), 3.62 (dd, *J* = 11.2, 5.7 Hz, 1H), 3.48 (dd, *J* = 9.1, 1.3 Hz, 1H), 2.22 (dd, *J* = 12.9, 4.9 Hz, 1H), 2.02 (s, 3H), 1.89 (dd, *J* = 12.8, 11.5 Hz, 1H); ¹³C {¹H}-NMR (101 MHz, CD₃OD) δ 175.10, 171.75, 96.66, 72.07, 71.64, 70.18, 67.84, 64.83, 54.31, 53.14, 40.69, 22.66.

4-Acetoxy-5-acetylamino-2-chloro-6-(1,2,3-triacetoxy-propyl)-tetrahydro-pyran-2-carboxylic acid methyl ester (12b) was synthesized based on a literature procedure.³ Ester 12a (2.00 g, 6.19 mmols) was added to a stirred solution of fresh acetyl chloride (50 mL) and acetic acid (15 mL) cooled in a NaCl ice bath. The reaction mixture was left to warm to room temperature and stirred for 24 hrs. The excess acetyl chloride and acetic acid was then removed *in vacuo* at 40°C by co-evaporating with toluene. The crude mixture was subjected to flash chromatography (ethyl acetate) to afford the protected sialic acid 12b as a white foam (1.97 g, 62%). The proton and carbon NMR confirmed the presence of protected 12b in >80 % purity. It was used in the next step without further purification.

¹H-NMR (400 MHz, CDCl₃) δ 5.94 (d, *J* = 10.1 Hz, 1H), 5.44 (dd, *J* = 6.6, 2.4 Hz, 1H), 5.40 – 5.32 (m, 1H), 5.13 (td, *J* = 6.3, 2.7 Hz, 1H), 4.41 (dd, *J* = 12.5, 2.7 Hz, 1H), 4.34 (dd, *J* = 10.8, 2.4 Hz, 1H), 4.18 (q, *J* = 10.4 Hz, 1H), 4.03 (dd, *J* = 12.5, 6.2 Hz, 1H), 3.83 (s, 3H), 2.74 (dd, *J* = 13.9, 4.8 Hz, 1H), 2.22 (dd, *J* = 13.9, 11.2 Hz, 1H), 2.08 (s, 3H), 2.04 (s, 3H), 2.01 (d, *J* = 1.0 Hz, 6H), 1.86 (s, 3H); ¹³C {¹H}-NMR (101 MHz, CDCl₃) δ 170.99, 170.70, 170.50, 170.00, 169.89, 165.68, 96.73, 74.03, 70.26, 68.86, 67.03, 62.20, 53.84, 48.64, 40.71, 23.13, 20.98, 20.89, 20.83, 20.80.

4-Acetoxy-5-acetylamino-2-but-3-ynyloxy-6-(1,2,3-triacetoxy-propyl)-tetrahydro-pyran-2-carboxylic acid methyl ester (12d) was synthesized based on a modified procedure.⁴ The protected sialic acid 12b (1.59 g, 3.11 mmols, 1 eq) and 4Å molecular sieves (4.00 g) were evacuated and back filled with nitrogen 3 times. 3-Butyn-1-ol, 12c (1.60 mL, 21.8 mmols, 7 eq) and anhydrous acetonitrile (50 mL) was then added under N₂ atmosphere and stirred at room temperature. After 1 hr, silver triflate (2.40 g, 9.36 mmol, 3 eq) was added and the resulting reaction was left to stir in the dark at 40°C for 24 hrs. The resulting suspension was filtered, concentrated *in vacuo* at 40 °C and reconstituted in CHCl₃ (100 mL). The organic mixture was later washed with sat. NaHCO₃ (100 mL), brine (100 mL), dried over Na₂SO₄ and concentrated *in vacuo* at 40 °C. The crude mixture was purified using flash chromatography (3 % MeOH in DCM) to give a mixture of α and β 12d as an off-white foam (58 %, 945 mg)

in approximate 65 % purity. The product 12d was used without further purification in the next step.

TLC (MeOH:DCM, 3:97 v/v): $R_F = 0.28$; $^1\text{H-NMR}$ (400 MHz, CD_3OD) δ 5.41 (dd, $J = 5.3$, 2.1 Hz, 1H), 5.40 – 5.36 (m, 1H), 5.33 (d, $J = 2.1$ Hz, 1H), 5.32 – 5.27 (m, 1H), 5.21 (td, $J = 11.2$, 4.9 Hz, 1H), 4.81 (dd, $J = 4.5$, 1.6 Hz, 2H), 4.73 (dd, $J = 12.4$, 2.5 Hz, 1H), 4.31 (dd, $J = 12.4$, 2.6 Hz, 1H), 4.22 (dd, $J = 10.6$, 2.1 Hz, 1H), 4.15 (dd, $J = 10.8$, 2.0 Hz, 1H), 4.13 – 4.06 (m, 2H), 4.04 – 3.92 (m, 2H), 3.87 – 3.85 (m, $J = 6.7$ Hz, 1H), 3.83 (s, 3H), 3.81 (s, 3H), 3.66 – 3.56 (m, 1H), 3.53 – 3.43 (m, $J = 9.1$, 6.2 Hz, 1H), 3.43 – 3.34 (m, $J = 9.4$, 7.0 Hz, 1H), 2.64 (dd, $J = 12.7$, 4.6 Hz, 1H), 2.54 – 2.45 (m, 3H), 2.41 (ddd, $J = 12.7$, 6.9, 4.0 Hz, 4H), 2.27 (t, $J = 2.6$ Hz, 1H), 2.14 (s, 3H), 2.11 (s, 6H), 2.07 (s, 3H), 2.01 (s, 6H), 1.99 (s, 3H), 1.98 (s, 4H), 1.85 (s, 3H), 1.84 (s, 3H), 1.83 – 1.81 (m, 1H); ^{13}C $\{^1\text{H}\}$ -NMR (101 MHz, CD_3OD) δ 173.40, 173.36, 172.31, 172.28, 171.91, 171.81, 171.71, 171.62, 171.50, 171.45, 169.45, 168.76, 100.05, 99.88, 81.82, 81.63, 73.23, 72.54, 72.23, 71.51, 70.68, 70.62, 70.34, 69.57, 69.44, 68.57, 64.35, 63.48, 63.38, 63.34, 53.32, 53.31, 50.07, 50.02, 38.94, 38.35, 22.70, 22.65, 21.23, 21.14, 20.87, 20.82, 20.80, 20.74, 20.69, 20.61, 20.28; LRMS (m/z): $[\text{M}]^+$ calcd for $\text{C}_{24}\text{H}_{33}\text{NO}_{13}$, 543.52, found 543.86.

5-Acetylamino-2-but-3-ynoxy-4-hydroxy-6-(1,2,3-trihydroxy-propyl)-tetrahydro-pyran-2-carboxylic acid methyl ester (12e) was synthesized based on the modified literature procedure.^{3,4} Alkyne 12d (829 mg, 1.53 mmols) was stirred in NaOMe in MeOH (0.5 M, 0.8 mL) and anhydrous MeOH (20 mL) for 24 hrs. The resulting reaction was neutralized using Amberlite IR 120 (H^+) and filtered. The filtrate was concentrated *in vacuo* at 40°C and purified using flash chromatography (13% to 20% MeOH in CH_2Cl_2) to give the α and β product 12e as an off-white foam (166 mg, 29 %).

TLC (EtOAc): $R_F = 0.28$; $^1\text{H-NMR}$ (400 MHz, CD_3OD) δ 3.92 – 3.78 (m, 8H), 3.75 (d, $J = 10.2$ Hz, 1H), 3.69 – 3.61 (m, 3H), 3.57 (dd, $J = 10.4$, 1.7 Hz, 1H), 3.55 – 3.48 (m, 3H), 2.69 (dd, $J = 12.8$, 4.7 Hz, 1H), 2.44 – 2.38 (m, 3H), 2.26 (t, $J = 2.7$ Hz, 1H), 2.00 (s, 3H), 1.73 (dd, $J = 12.8$, 11.8 Hz, 1H); ^{13}C $\{^1\text{H}\}$ -NMR (101 MHz, CD_3OD) δ 175.19, 170.84, 100.22, 81.50, 74.95, 72.39, 70.60, 70.17, 68.51, 64.75, 63.72, 53.79, 53.40, 41.62, 22.66, 20.63; analysis (% calcd, % found for $\text{C}_{16}\text{H}_{25}\text{NO}_9$): C (51.20, 51.16), H (6.71, 6.74), N (3.73, 3.60)

α -alkyne sialic acid (13) was synthesized based on a modified literature procedure.³ Ester 12e (540 mg, 1.44 mmols) in aqueous NaOH solution (0.2M, 8 mL) was stirred at room

temperature for 24 hrs. The resulting solution was neutralized using amberlyst IR-120 (H^+), filtered and purified using flash chromatography (DCM/MeOH/ H_2O , 65:35:0.5) to give the α -product 13 as an off-white solid (112 mg, 22 %). The α -anomer was confirmed using 1H -NMR.³

TLC (EtOAc:*i*PrOH: H_2O , 2:2:1 v/v): $R_F = 0.5$; 1H -NMR (400 MHz, CD_3OD) δ 3.90 – 3.80 (m, 3H), 3.74 – 3.54 (m, 6H), 3.49 (dd, $J = 9.1, 1.8$ Hz, 1H), 2.83 (dd, $J = 12.3, 4.3$ Hz, 1H), 2.41 (td, $J = 7.6, 2.6$ Hz, 2H), 2.19 (d, $J = 2.7$ Hz, 1H), 2.01 (s, 3H), 1.62 – 1.50 (m, 1H); ^{13}C { 1H }-NMR (101 MHz, CD_3OD) δ 175.55, 174.21, 101.91, 81.70, 74.40, 72.95, 70.39, 70.34, 69.48, 64.49, 63.75, 54.20, 42.71, 22.57, 20.77; HRMS (m/z): $[M+Na]^+$ calcd for $C_{15}H_{21}DNNaO_9$, 384.1254; found, 384.1279.

1.5 Synthesis of sialic acid terminated amphiphile (2)

4-(10-(4-(2-(2-(2-chloroethoxy)ethoxy)ethyl)phenoxy)decyloxy)benzotrile (9) was synthesized based on a modified literature procedure.⁵ Aqueous NaOH (50% w/w, 2.5 mL) was added to a stirred solution of nitrile 7 (200 mg, 0.51 mmols, 1 eq), tetrabutylammonium hydrogen sulfate (343 mg, 1.01 mmols, 2 eq) and 2-chloroethyl ether 8 (2.5 mL, 22 mmols, 43 eq) and left to stir at room temperature for 18 hrs. The resulting two-phase suspension was reconstituted in chloroform (15 mL) and washed with water (3×25 mL). The organic layer was dried over $MgSO_4$ and the excess solvent removed *in vacuo* at $40^\circ C$. Purification of the crude product using flash column chromatography (20 to 40 % ethyl acetate in hexane) afforded the chloride 9 as an amorphous white solid (143 mg, 56 %).

TLC (EtOAc:Hexane, 3:7 v/v): $R_F = 0.55$; 1H -NMR (400 MHz, $CDCl_3$) δ 7.57 (d, $J = 8.8$ Hz, 2H), 7.12 (d, $J = 8.5$ Hz, 2H), 6.93 (d, $J = 8.8$ Hz, 2H), 6.81 (d, $J = 8.5$ Hz, 2H), 3.95 (dt, $J = 27.4, 6.5$ Hz, 4H), 3.73 (t, $J = 5.9$ Hz, 2H), 3.70 – 3.54 (m, 8H), 2.84 (t, $J = 7.3$ Hz, 2H), 1.92 – 1.70 (m, 4H), 1.38 (d, $J = 48.3$ Hz, 12H); ^{13}C { 1H }-NMR (101 MHz, $CDCl_3$) δ 162.53, 157.68, 134.08, 130.75, 129.93, 119.52, 115.25, 114.42, 103.65, 72.75, 71.47, 70.73, 70.34, 68.48, 68.02, 42.87, 35.43, 29.59, 29.57, 29.49, 29.41, 29.07, 26.17, 26.03 LRMS (m/z): $[M+Na]^+$ calcd for 525.08, found 524.26, 526.26.

Amino(4-(10-(4-(2-(2-(2-chloroethoxy)ethoxy)ethyl)phenoxy)decyloxy)phenyl)methan iminium chloride (10) was synthesized based on a modified literature procedure.² HCl gas (150 ml of sulfuric acid to 135 g of NaCl) was bubbled into a stirred solution of 9 (1 g, 1.99 mmols, 1 eq) in MeOH, anhydrous (50mL) cooled in a NaCl-ice bath. After the bubbling had ceased, the reaction was warmed to room temperature and left to stir for 24 hrs. The excess solvent was removed *in vacuo* and methanolic NH₃ (7 N, 50 mL) was added. The reaction mixture was further stirred at room temperature for 24 hrs. The resulting product was then concentrated and recrystallized in 1M HCl in EtOH to give the amidine 10 as an off-white amorphous solid (0.59 g, 53 %).

¹H-NMR (400 MHz, DMSO) δ 9.20 (s, 2H), 8.96 (s, 2H), 7.83 (d, *J* = 8.7 Hz, 2H), 7.20 – 7.04 (m, 4H), 6.87 – 6.74 (m, 2H), 4.07 (t, *J* = 6.5 Hz, 2H), 3.90 (t, *J* = 6.5 Hz, 2H), 3.72 – 3.60 (m, 4H), 3.53 (tdd, *J* = 5.8, 4.8, 2.4 Hz, 6H), 2.72 (t, *J* = 7.0 Hz, 2H), 1.79 – 1.59 (m, 4H), 1.49 – 1.20 (m, 12H). ¹³C-NMR (101 MHz, DMSO) δ 164.69, 163.06, 157.01, 130.65, 130.13, 129.71, 119.20, 114.72, 114.13, 71.53, 70.52, 69.61, 69.45, 68.07, 67.27, 43.56, 34.63, 28.91, 28.91, 28.73, 28.70, 28.43, 25.51, 25.38. LRMS (*m/z*): [M]⁺ calcd for 520.12, found 519.62, 521.6165.

Amino(4-(10-(4-(2-(2-(2-azidoethoxy)ethoxy)ethyl)phenoxy)decyloxy)phenyl)methan iminium azide (11) was synthesized based on a modified procedure.⁶ Chloride 10 (248 mg, 0.48 mmols, 1.0 eq), sodium azide (124 mg, 1.91 mmols, 4.0 eq.) in DMF, anhydrous (4 mL) was stirred at 60°C, N₂ for 24 hrs. The crude reaction mixture was then concentrated *in vacuo*, dissolved in chloroform and filtered. The filtrate was purified using flash chromatography (10% MeOH in DCM) to give the product as an off-white amorphous solid (127 mg, 47%). The product was acidified with 1M HCl in methanol before the next step.

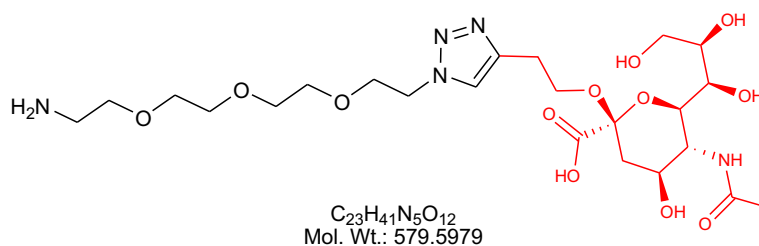
TLC (MeOH:DCM, 1:9 v/v): *R*_F = 0.43; ¹H-NMR (400 MHz, CD₃OD) δ 7.82 – 7.74 (m, 2H), 7.15 – 7.08 (m, 4H), 6.83 – 6.77 (m, 2H), 4.09 (t, *J* = 6.4 Hz, 2H), 3.93 (t, *J* = 6.4 Hz, 2H), 3.71 – 3.55 (m, 8H), 3.33 (d, *J* = 5.2 Hz, 2H), 2.79 (t, *J* = 7.0 Hz, 2H), 1.86 – 1.69 (m, 4H), 1.55 – 1.31 (m, 12H); ¹³C{¹H}-NMR (101 MHz, CD₃OD) δ 167.62, 165.49, 159.03, 132.23, 131.03, 130.85, 120.64, 116.20, 115.40, 73.57, 71.47, 71.37, 71.12, 69.66, 68.97, 51.77, 36.30, 30.58, 30.57, 30.44, 30.43, 30.38, 30.13, 27.15, 27.03; HRMS (*m/z*): [M]⁺ calcd for C₂₉H₄₄N₅O₄⁺, 526.3393, found 526.3395.

5-Acetylamino-2-[2-(1-{2-[2-(2-{4-[10-(4-carbamimidoyl-phenoxy)-decyloxy]-phenyl}-ethoxy)-ethoxy]-ethyl}-1H-[1,2,3]triazol-4-yl)-ethoxy]-4-hydroxy-6-(1,2,3-trihydroxy-

propyl)-tetrahydro-pyran-2-carboxylic acid (2). Amidine azide precursor 11 (74 mg, 0.13 mmol, 1 eq), α -linked alkyne sialic acid 13 (47 mg, 0.13 mmol, 1 eq), sodium ascorbate (77 mg, 0.39 mmol, 3 eq) and copper (II) sulphate (19 mg mmol, 0.3 eq) in water/2-butanol (1:2, 1 mL) was sonicated and stirred at room temperature for 4 hrs. The reaction mixture was concentrated *in vacuo* and purified using C18 flash chromatography (35% AcCN, 0.1% TFA in H₂O). The purified fractions were then concentrated *in vacuo* at 30°C and the residual water was lyophilized to give the TFA salt of sialic acid terminated amphiphile 2 as an amorphous white powder (69 mg, 60 %).

HPLC (C-18 column, mobile phase: 10% - 90 % ACN (0.1% TFA) in water (0.1% TFA) (0-30 mins) 90% ACN in water (30-35 mins)): $k=10.6$ (see chromatogram in Supplementary section 3). ¹H-NMR (400 MHz, CD₃OD) δ 7.86 (s, 1H), 7.80 – 7.73 (m, 2H), 7.10 (dt, $J = 3.4, 2.2$ Hz, 4H), 6.82 – 6.76 (m, 2H), 4.48 (t, $J = 5.1$ Hz, 2H), 4.08 (t, $J = 6.4$ Hz, 2H), 4.02 (s, 1H), 3.91 (t, $J = 6.4$ Hz, 2H), 3.86 – 3.80 (m, 3H), 3.80 – 3.66 (m, 4H), 3.65 – 3.46 (m, 10H), 2.92 (d, $J = 6.0$ Hz, 2H), 2.79 – 2.67 (m, 3H), 2.00 (s, 3H), 1.86 – 1.67 (m, 5H), 1.55 – 1.30 (m, 12H); ¹³C{¹H}-NMR (101 MHz, CD₃OD) δ 175.34, 167.65, 165.49, 159.02, 132.26, 131.03, 130.88, 120.69, 116.21, 115.42, 75.03, 73.46, 72.82, 71.44, 71.32, 70.40, 70.12, 69.65, 68.97, 68.72, 64.57, 63.99, 53.89, 51.38, 49.85, 49.71, 49.50, 49.28, 41.84, 36.29, 30.56, 30.54, 30.42, 30.36, 30.11, 27.31, 27.14, 27.02, 22.63; HRMS (m/z): [M]⁺ calcd for C₄₄H₆₇N₆O₁₃, 887.4766, found 887.4788

1.6 Synthesis and sialic acid tether (14) for covalent immobilization



14

Alkyne sialic acid **13** (20 mg, 0.055 mmol, 1 eq) and 11-Azido-3,6,9-trioxaundecan-1-amine (11 μ L, 0.055 mmol, 1 eq) were dissolved in butanol:water (2:1, 900 μ L). Ascorbic acid (sodium salt) (1.1 mg, 5.5×10^{-3} mmol, 0.1 eq) and Cu(II) sulphate hydrate (0.14 mg, 5.5×10^{-4} mmol, 0.01 eq) predissolved in butanol:water (2:1, 100 μ L) was added. The reaction mixture

was stirred at 40°C for 2 hrs. The crude mixture was then dried *in vacuo* at 40°C and methanol (1 mL) was added. The MeOH mixture was left in the freezer for 1 hr and the resulting precipitate was centrifuged and the supernatant was collected and dried. The dried filtrate was redissolved in water and passed through a C18 column. The collected monolayer was dried *in vacuo* to give **14** as a light yellow solid (27 mg, 84%).

¹H NMR (400 MHz, CD₃OD) δ 7.99 (s, J = 16.3 Hz, 1H), 4.55 (t, J = 5.1 Hz, 2H), 4.05 (dd, J = 16.1, 6.7 Hz, 1H), 3.90 (t, J = 5.1 Hz, 2H), 3.83 (dt, J = 6.5, 2.5 Hz, 2H), 3.79 – 3.53 (m, 17H), 3.49 (dd, J = 8.9, 1.6 Hz, 1H), 2.94 (t, J = 6.5 Hz, 2H), 2.84 (dd, J = 12.4, 4.1 Hz, 1H), 2.02 (s, J = 7.7 Hz, 3H), 1.59 (t, J = 11.6 Hz, 1H). ¹³C NMR (101 MHz, CD₃OD) δ 175.56, 124.85, 74.44, 73.14, 71.60, 71.56, 71.54, 71.48, 71.47, 71.39, 71.24, 71.08, 70.43, 70.36, 69.46, 64.67, 63.83, 54.24, 51.76, 51.26, 42.73, 27.50, 22.59. ESI-MS (M-H)⁻: calculated 578.2679; found: 578.3762

1.7 Kinetic interaction analysis

In situ ellipsometry, in analogy with surface plasmon resonance (SPR), allows real time monitoring of adsorption and desorption events at solid surfaces. The latter technique has been extensively used to analyse ligand-receptor association dissociation kinetics and for assessing binding constants.⁷ We have here used the former technique for the same purpose.

Under pseudo first order conditions where the free target concentration is held constant in the cuvette, the binding can be described by Eq. 1:

$$(1) \quad d\Gamma / dt = k_a C (\Gamma_{\max} - \Gamma) - k_d \Gamma$$

where Γ = the measured adsorbed amount per unit area (mg/m²), Γ_{\max} = the maximum adsorbed amount per unit area, C is the injected concentration (M) of the virus or protein, k_a is the association rate constant or on-rate (M⁻¹s⁻¹) and k_d is the dissociation rate or off-rate (s⁻¹). The dissociation constant may be calculated according to equation 2 as:

$$(2) \quad K_d = k_d / k_a (M)$$

Equation [1] may be rearranged as:

$$(3) \quad d\Gamma / dt = k_a C \Gamma_{\max} - (k_a C + k_d) \Gamma$$

thus plotting $d\Gamma/dt$ against Γ for each cycle of association dissociation (Supplementary Fig. 12B) give rise to straight lines with slope $S = k_a C + k_d$. A plot of S against C will in turn be a straight line with slope k_a (Supplementary Fig. 12C). The dissociation rate constant, k_d , was determined by the average of direct measurements of the dissociation from saturated binding sites into a buffer solution by nonlinear curve fitting to the dissociation rate equation (4) (Supplementary Figure 12D-G).

$$(4) \quad d\Gamma / dt = k_d \Gamma_0$$

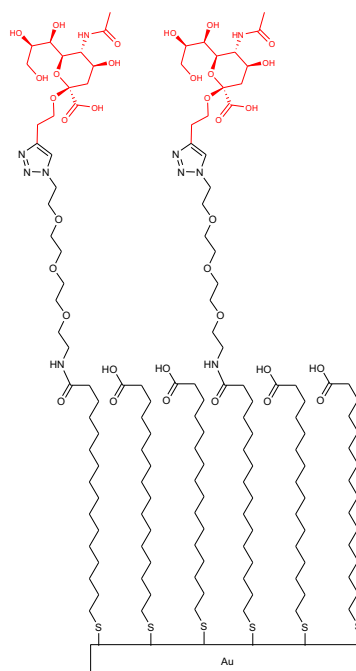
The result of the analysis is summarized in Supplementary Table 8.

1.8 Substrates

For ellipsometry, IRAS and contact angle, the gold surfaces were prepared by electron beam (e-beam) evaporation of gold (2000 Å thickness) onto precleaned glass slides (76 x 26 x 1 mm) containing adhesive layers (25 Å) of titanium. Prior to thiol adsorption, these gold surfaces were rinsed with ethanol, water and treated with plasma cleaner. Gold on mica for atomic force microscopy was purchased from Phasis and used without further processing. The MHA SAMs were prepared by immersing the cleaned or freshly prepared gold substrate in 1 mM 16-mercaptohexadecanoic acid (MHA) in ethanol (99.5%) for 12 hrs followed by rinsing with copious amount of ethanol and drying under a nitrogen stream.

The covalently anchored sialic acid monolayer the MHA functionalized slides were activated using 200 mM EDC and 50 mM NHS in water for 15 mins (see reference 8 of main manuscript). The slides were then rinsed thoroughly with water. The activated slides were then left in an aqueous solution of **14** (100 µM) at room temperature for 1.5 hrs. It was then rinsed again and the unreacted NHS-esters were then hydrolysed in 1 M NaOH solution for 15

mins. The final slides were then rinsed thoroughly with water. Immobilization of **14** was confirmed by contact angle, FTIR and ellipsometry. Ellipsometry suggested a surface coverage of **14** of 27 %.



Scheme 1. Schematic view of a covalently anchored mixed SAM of **14** and MHA on gold.

1.9 Infrared reflection-adsorption spectroscopy (IRAS)

The measurements were made using a Nicolet 6400 instrument equipped with a liquid nitrogen-cooled MCT-A detector operating at a resolution of 4 cm^{-1} . Data was collected with a smart Saga accessory operating at an angle of incidence of 80° . The instrument was purged with nitrogen before and during measurements. Each spectrum is the sum of 512 scans on the modified surfaces using an unreacted, cleaned gold substrate as reference. Each spectrum was processed using OMINIC software and baselined corrected.

1.10 Atomic Force Microscopy

The surfaces were modified as described in the experimental section using freshly deposited gold on mica and dried under a stream of nitrogen prior to measurement unless stated otherwise. The surfaces were examined with a commercial Atomic Force Microscope (AFM) (MultiMode 8 SPM with a NanoScope V control unit, Bruker AXS) in air at room temperature in PeakForce Tapping® mode. Cantilevers with nominal spring constant 0.5819 N m^{-1} were employed. Analysis and processing of AFM images were performed using the Gwyddion software.⁸ Each substrate was scanned at min. 2 points.

1.11 Contact Angle

A milli Q water droplet was formed at the end of the needle and lowered onto the surface. The needle was raised as soon as the water droplet touches the surface and the contact angle analysed using drop shape analysis was recorded immediately. Measurements were taken consecutively on different areas on the surface and averaged based on a minimum of 3 measurements.

2 Supplementary Tables

Table 1. Characterisation results of the SAMs in the study.

Self assembled monolayers					
	MHA	14 ^g	1	1+2 ($\chi_2 = 0.2$)	2
Contact Angle ($^\circ$) ^a	22±2	27±4	47±11	29±0	40±2
d (Å) ^b	21	26	28	-	47
d _{ads} (Å) ^c	-	-	44±0	58±0	54±1
d _{rinse} (Å) ^c	21±1	7±2 ^h	46±0	49±2	19±1
ν CH ₂ CH asym (cm ⁻¹) ^d	2920±1	2918	2929±1	2919±1	2923±1
ν CH ₂ CH sym (cm ⁻¹) ^d	2851±0	2850	2853±1	2851±1	2855±2
Tilt angle ($^\circ$) ^e	37±4	-	13±3	19±4	19±0
Roughness, R _{RMS} (nm) ^f	0.21 (0.01)	0.38 (0.04)	1.33 (0.02)	2.44 (0.30)	0.29 (0.05)

The surfaces were rinsed with pH 8 HEPES buffer (0.01 M) prior to analysis unless stated otherwise. All reported values are the average of min. 2 experiments on different substrates unless indicated otherwise.

^a The static contact angle was taken at 3 different positions as indicated in Supplementary section 1.11.

^b Theoretical film thickness (d) assuming a densely packed layer of molecules oriented perpendicularly to the surface with the alkyl chains in an all-*trans* arrangement.

^c Adsorbed thickness of MHA, d_{rinse} was estimated using *in situ* ellipsometry after the adsorption of MHA onto cleaned gold surfaces in EtOH and rinsing with EtOH. The adsorbed thickness, d_{ads} of rSAMs 1, 1+2 and 2 on MHA modified gold surfaces were estimated using *in situ* ellipsometry after the system reached steady state or for a maximum duration of 5000 s after introduction of the amphiphiles in pH 9 borate buffer (0.01 M). Thickness after rinsing, d_{rinse} of rSAMs 1, 1+2 and 2 were estimated after rinsing the surfaces with pH 8 HEPES buffer (0.01 M) for 1000 s followed by equilibration until steady state or for a maximum duration of 5000 s. The thickness values were calculated as indicated in the Methods Section.

^d IR band positions corresponding to the CH₂ C-H asym and CH₂ C-H sym stretch of the spectra in Figure 3 and Supplementary Figure 3.

^e The average tilt angles, θ of the phenyl group relative to the surface perpendicular for rSAMs adsorbed on MHA. The tilt angles were calculated on the basis of the relative intensity of the bands corresponding to two perpendicular ring modes - the (C=C)_{1,4} stretch band at 1611 cm⁻¹ and the C-H

out-of plane bending mode at ca. 843 cm⁻¹. The spectra were subjected to base-line correction prior to analysis. See references 20 and 21 of the main manuscript.

^f The roughness, R_{RMS} was calculated based on the 500 μm x 500 μm area indicated in Figure 3 using Gwyddion. Each substrate was sampled in two areas. The bracketed values indicate the standard deviation.

^g Results for the covalently anchored sialic acid SAM (SAM-14).

^h Results from ex-situ ellipsometry in air.

Table 2. Positions and spectral mode assignments of the IR bands of 1 shown in Fig 3.

Mode assignment	Monolayer	Bulk (Crystalline)
NH ₂ , N-H stretch (asym)	3344	3286
CH ₂ , C-H stretch (asym)	2929	2921
CH ₂ , C-H stretch (sym)	2853	2849
Amidinium ion, N-C=N stretch (asym)	1692	1684
Aromatic C=C stretch (1,4 axis)	1612 / 1514	1606 / 1511
Aromatic C=C stretch (1,4 axis)	1435	-
Aromatic ethers, aryl-O stretch (asym)	1247	1236
Aromatic ethers, O-CH ₂ stretch	1044	1036
1° OH, C-C-O stretch (out of phase)		
Aromatic C-H stretch (out of plane)	844	845

Table 3. Positions and spectral mode assignments of the IR bands of 2 shown in Fig 3. Modes highlighted in red are functionalities present in the sialic acid head group.

Mode Assignment(s)	Monolayer	Bulk (Amorphous)
NH ₂ , N-H stretch (asym)	3345	3325
CONH, N-H stretch (trans)		
COOH, OH, Hydrogen-Bonded OH stretch		
CH ₂ , C-H stretch (asym)	2923	2929
CH ₂ , C-H stretch (sym)	2855	2857
Amidinium ion, N-C=N stretch (asym)	1694	1666
COOH, CONH, C=O stretch		
Aromatic C=C stretch (1,4 axis)	1611	1611
	1513	1512
Aromatic C=C stretch (1,4 axis)	1431	1437
COO-, COOH, C-OH bend (in plane)		
Aromatic ethers, aryl-O stretch (asym)	1246	1244
Aliphatic ethers, C-O-C stretch (asym)	1115	1129
2° OH, C-C-O stretch (out of phase)		
Aromatic ethers, O-CH ₂ stretch	1041	1033
1° OH, C-C-O stretch (out of phase)		
Aromatic C-H stretch (out of plane)	837	840

Table 4. Normalized peak area ratio (A_{obs}/A_{1611}) of characteristic sialic acid IR spectral bands of rSAMs prepared from 1, 2 or 1+2 as shown in Supplementary Fig. 3. The bands peak areas are normalized against the aromatic C=C stretch ($\parallel 1,4$ axis) at 1611 cm^{-1} .

IR mode assignment	Frequency (cm^{-1})	A_{obs}/A_{1611}		
		rSAM-1	rSAM-1+2 ($\chi_2 = 0.2$)	rSAM-2
CONH, N-H stretch (trans) COOH, OH, OH stretch	3345	2.1 \pm 0.8	3.3 \pm 0.5	3.3 \pm 0.4
COOH, CONH, C=O stretch	1694	0.82 \pm 0.25	0.90 \pm 0.26	1.5 \pm 0.4
COO-, COOH, C-OH bend (in plane)	1431	0.48 \pm 0.14	1.0 \pm 0.2	1.6 \pm 0.2
aliphatic ethers, C-O-C stretch (asym) 2° OH, 3° OH, C-C-O stretch (out of phase)	1115	0.06 \pm 0.01	0.15 \pm 0.01	0.50 \pm 0.08

Table 5. Positions and spectral mode assignments of the IR bands of the spectra shown in Supplementary Fig 4. of 14 and the MHA-SAM after modification with 14. Modes highlighted in red are functionalities present in the sialic acid head group.

Mode assignments	14	Monolayer
CONH, N-H stretch (trans)	3254	3369
COOH, OH, Hydrogen-Bonded OH stretch,		
CH ₂ , C-H stretch (asym)		2918
CH ₂ , C-H stretch (sym)		2850
COOH Dimer CO ₂ ⁻	2877	
COOH		1728
NH ₂ CO ₂ ⁻	1602	1611
CO ₂ ⁻ OCN monosub amide	1559	1556 1510
COOH dimer CO ₂ ⁻	1436	1408
CO ₂ ⁻	1374	
COOH Dimer	1319	
COOH Dimer	1288	1292
C-O-C, Aliphatic ether C-O-H, Aliphatic Sec and Tert Alcohol	1109	1183
C-OH, Primary Alcohol	1070	1076
C-OH, Primary Alcohol, Cyclic Axial Secondary Alcohol	1028	1000
COOH Dimer	942	923
COOH Dimer	902	

Table 6. Properties of proteins used to probe sensor affinity and selectivity.

	Hemagglutinin (HA)	Concanavalin A (ConA)	Human Serum Albumin (HSA)	Mucin
Mw (Da)	59 000 ^a	102 000 ^b	66 500	0.5 – 250 x 10 ⁶
Dimensions (Å)	135 x (15-40) x (15-40)	42 x 40 x 39 ^c	80 x 80 x 30	-
pI	6.0-7.8	4.5-5.5	4.7	2.0-3.0
Ligand	α -1,3 or α -1,6 linked sialic acid	α -Mannose/ α -Glucose	-	Hemagglutinin

- a) Molecular weight of the homotrimeric form
- b) Molecular weight of the homotetrameric form
- c) Dimension of one subunit.

Table 7. Limits of detection (LoD), dissociation constant (K_d^{multi}) and curve fitting parameters for the adsorption isotherms in Figure 4.

	HA	ConA	HSA	H5N1
LoD	0.84 nM	-	-	0.5 HAU /46 fM
K_d^{multi} (M)	$5.1 \pm 0.4 \times 10^{-9}$	$60 \pm 6 \times 10^{-9}$	$1.1 \pm 0.5 \times 10^{-9}$	$2.3 \pm 0.1 \times 10^{-13}$
Γ_{max} (mg m ⁻²)	0.92 ± 0.02	1.6 ± 0.1	0.087 ± 0.007	1.83 ± 0.02
h	1.5 ± 0.2	1.0	1.0	2.2 ± 0.1
R ²	0.9992	0.9981	0.7366	0.9991

The data sets were analyzed and fitted with the empirical Hill equation generating an equilibrium dissociation constant calculated on the basis of multimeric species, K_d^{multi} , maximum specific binding, Γ_{max} , a Hill slope, h, and a correlation coefficient R². The limit of detection (LoD) was estimated as the concentration producing a signal corresponding to a minimum of three times the standard deviation (SD) of the blank signal (SD=0.017).

Table 8. Kinetic interaction analysis for the adsorption of HA and H5N1 on an rSAM-2.

	HA	H5N1
k_a	$1.6 \pm 0.03 \times 10^4$	$1.7 \pm 0.2 \times 10^9$
k_d	$1.4 \pm 0.02 \times 10^{-4}$	$2.0 \pm 0.5 \times 10^{-4}$
K_d^{multi}	$8.9 \pm 0.3 \times 10^{-9}$	$1.2 \pm 0.5 \times 10^{-13}$
R ²	0.9738	0.9756

3 Supplementary Figures

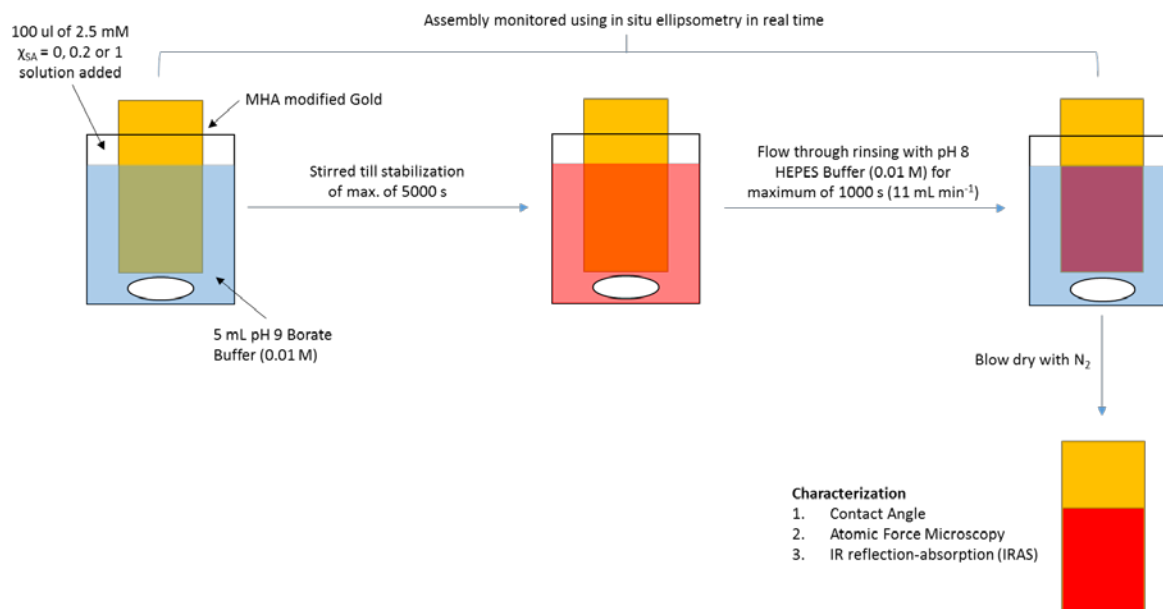


Figure 1. General protocol for rSAM characterization.

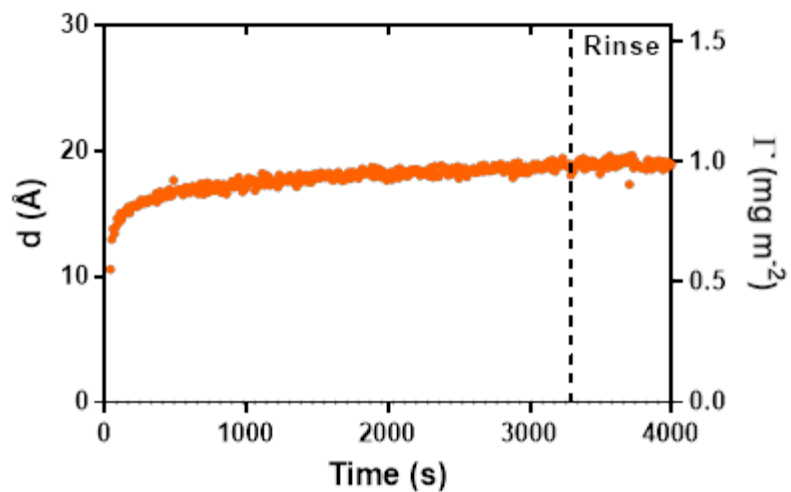


Figure 2. Film thickness, (d), and amount adsorbed, (Γ) estimated by in situ ellipsometry, versus time during adsorption of MHA (1 mM in ethanol) on gold assuming a film refractive index n_f of 1.5.

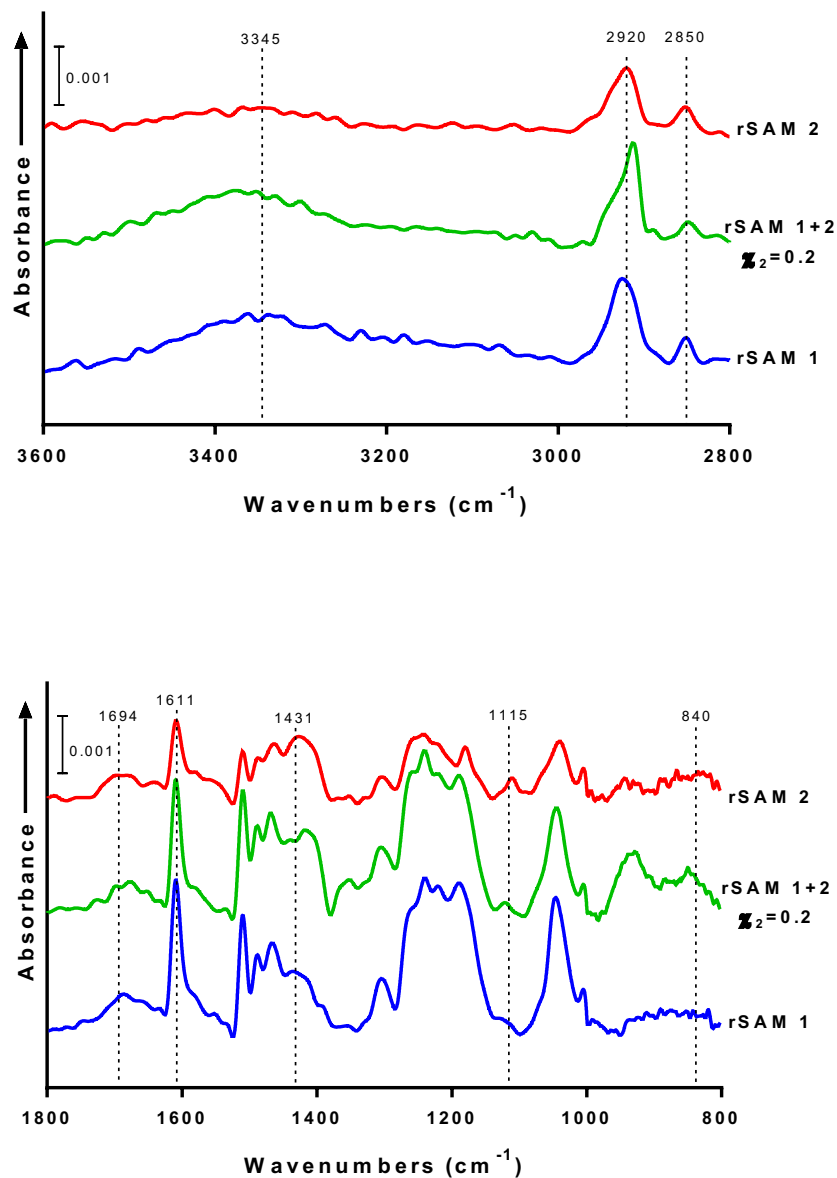


Figure 3. High frequency (top) and low frequency (bottom). IRAS spectra of rSAM-1, rSAM-2 or rSAM-1+2 ($\chi_2 = 0.2$) adsorbed on a SAM of MHA on gold at pH 9 followed by rinsing with pH 8 HEPES buffer.

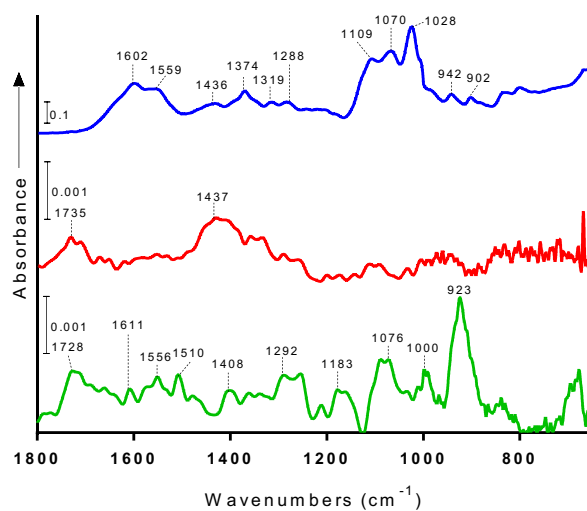
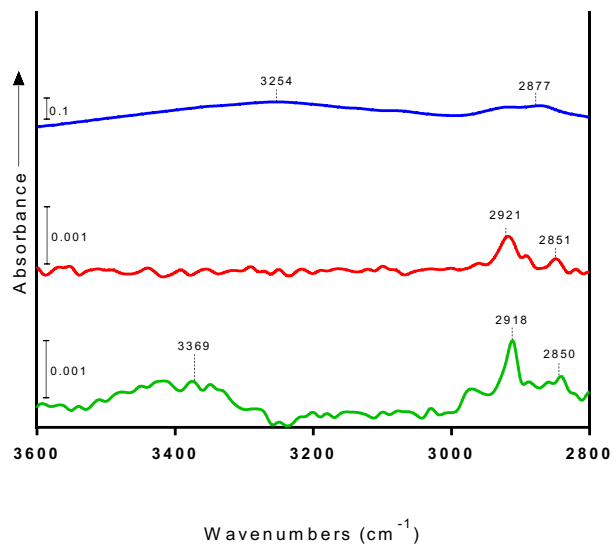


Figure 4. High frequency (top) and low frequency (bottom). IRAS spectra of neat 14 (top) and a SAM of MHA on gold prior to (middle spectrum) and after (bottom) modification with 14 as described in section 1.6.

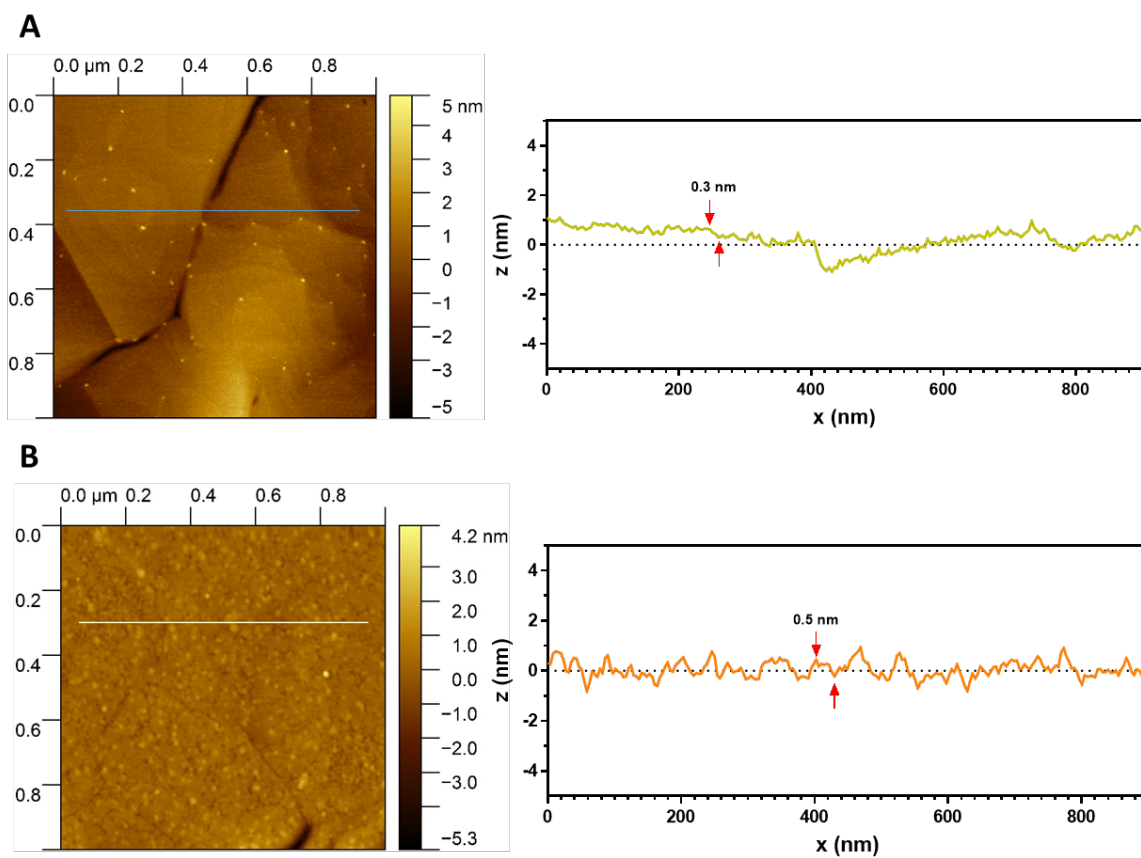


Figure 5. Topographical atomic force microscopy (AFM) images ($1\ \mu\text{m} \times 1\ \mu\text{m}$) of (A) a bare gold mica surface and (B) a SAM of MHA on gold after modification with 14. The images were obtained in quantitative nanoscale mechanical (QNM) mode in air. The peaks are obtained from a section analysis as indicated by the red arrows.

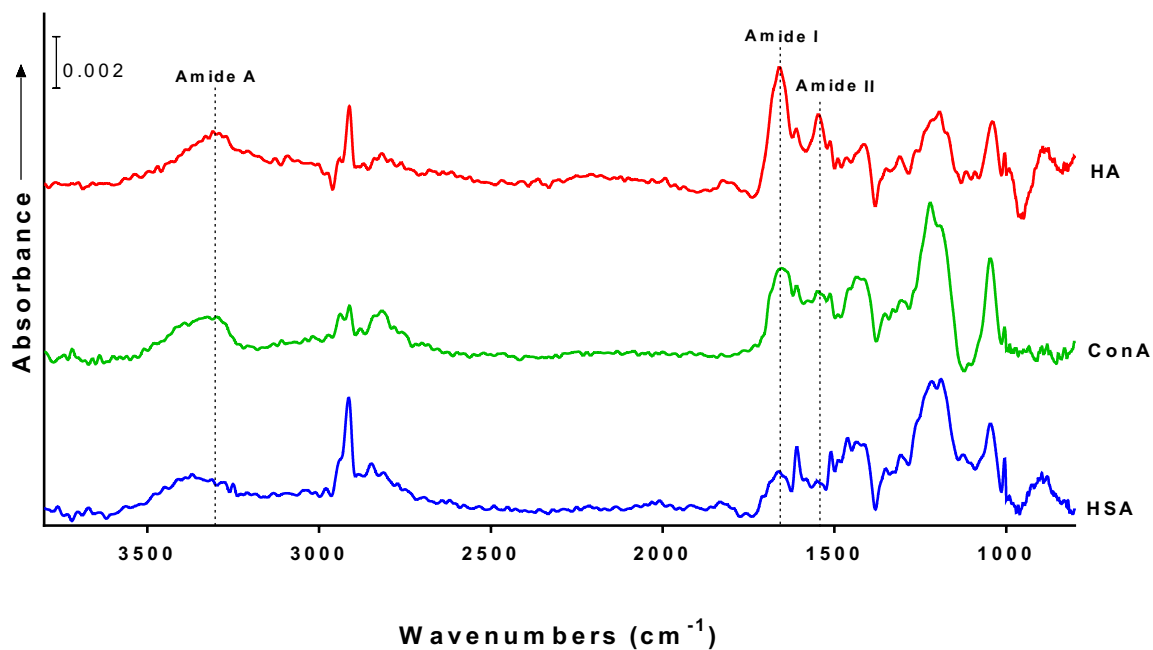


Figure 6. Baseline corrected IRAS of rSAM-2 on MHA modified gold after exposure to HSA (blue spectrum), ConA (green spectrum) and HA (red spectrum) (84 nM) followed by rinsing with pH 8 HEPES buffer. The indicated bands at around 3300 cm⁻¹, 1670 cm⁻¹ and 1560 cm⁻¹ are assigned to amide A, amide I and amide II vibrations of the protein respectively.

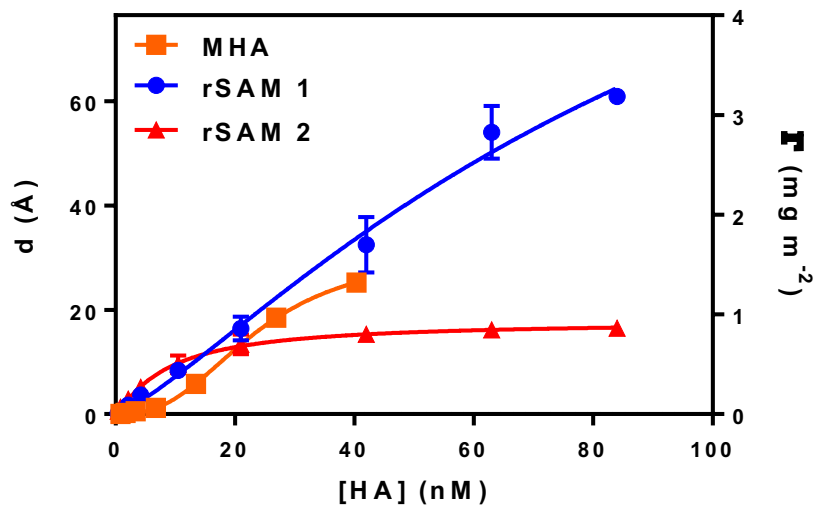


Figure 7. Film thickness, (d), and adsorbed amount, (Γ) estimated by ellipsometry for MHA, rSAM-1 or rSAM-2 on MHA modified gold upon addition of incremental amounts of hemagglutinin (HA) (0.42 – 84 nM).

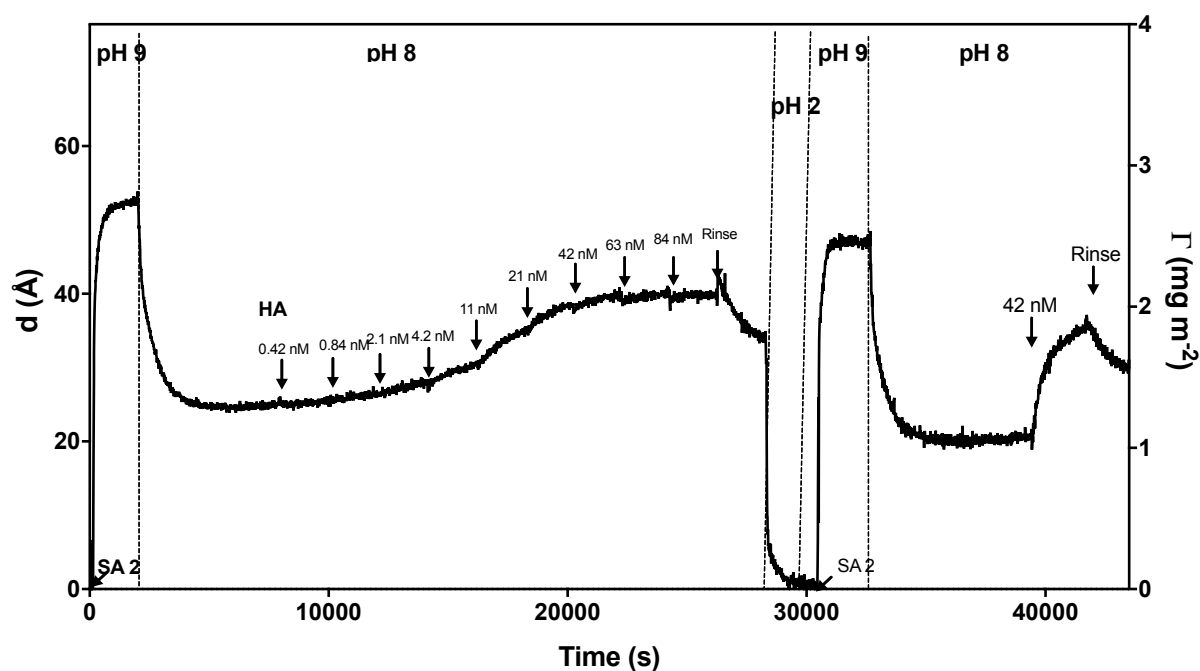
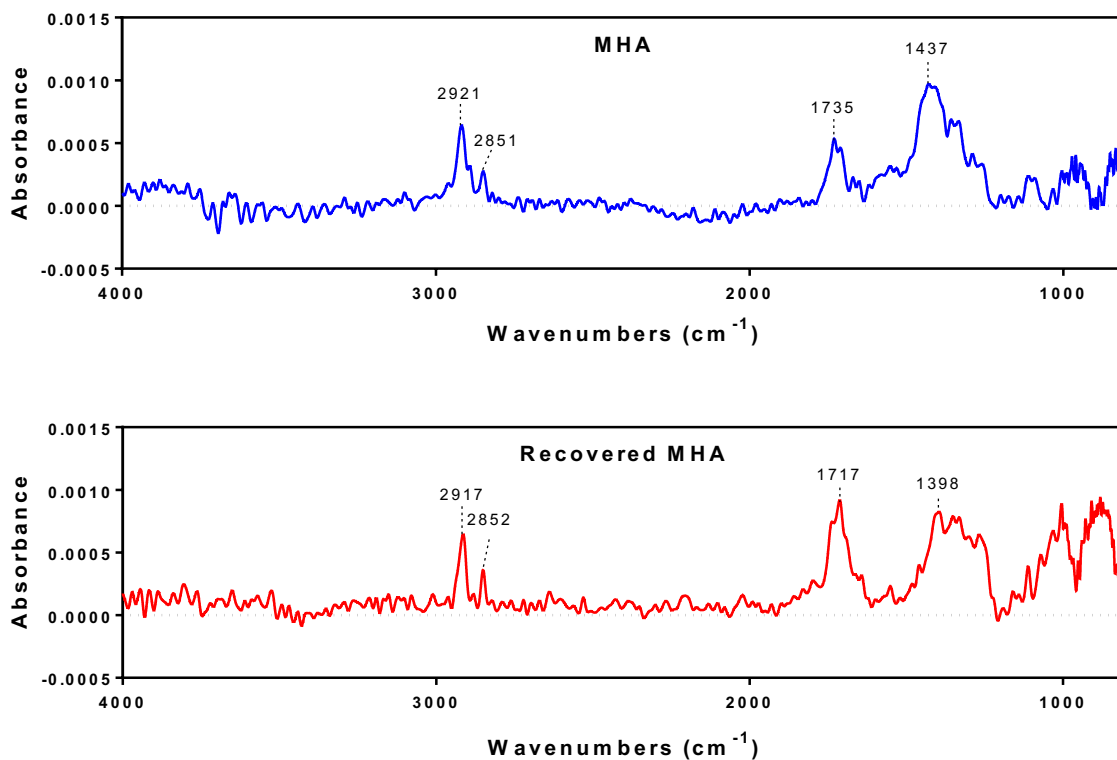


Figure 8. Film thickness, (d), and amount adsorbed, (Γ) estimated by *in situ* ellipsometry, versus time showing restorability of rSAM 2 modified with HA (0.42 to 84 nM) with pH cycling. Arrows indicate time of addition of 2 or HA or buffer rinse. The final concentration of HA in the system is indicated above the arrows. The pH of the system at the given time is printed at the top of the plot. The pH of the system was changed by continuous rinsing with the corresponding buffer.





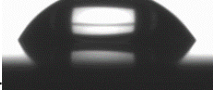

Sample	Contact Angle (°)
MHA	22±2 
Recovered MHA	23±1 
Amidine sialic acid with H5N1	54±4 
Amidine sialic acid with HA	49±1 

Figure 9. Restorability of rSAM-2 on MHA modified gold surfaces. IRAS of fresh and recovered MHA (top). Contact angle of MHA, Recovered MHA and after deposition of H5N1 or HA onto rSAM-2 (bottom).

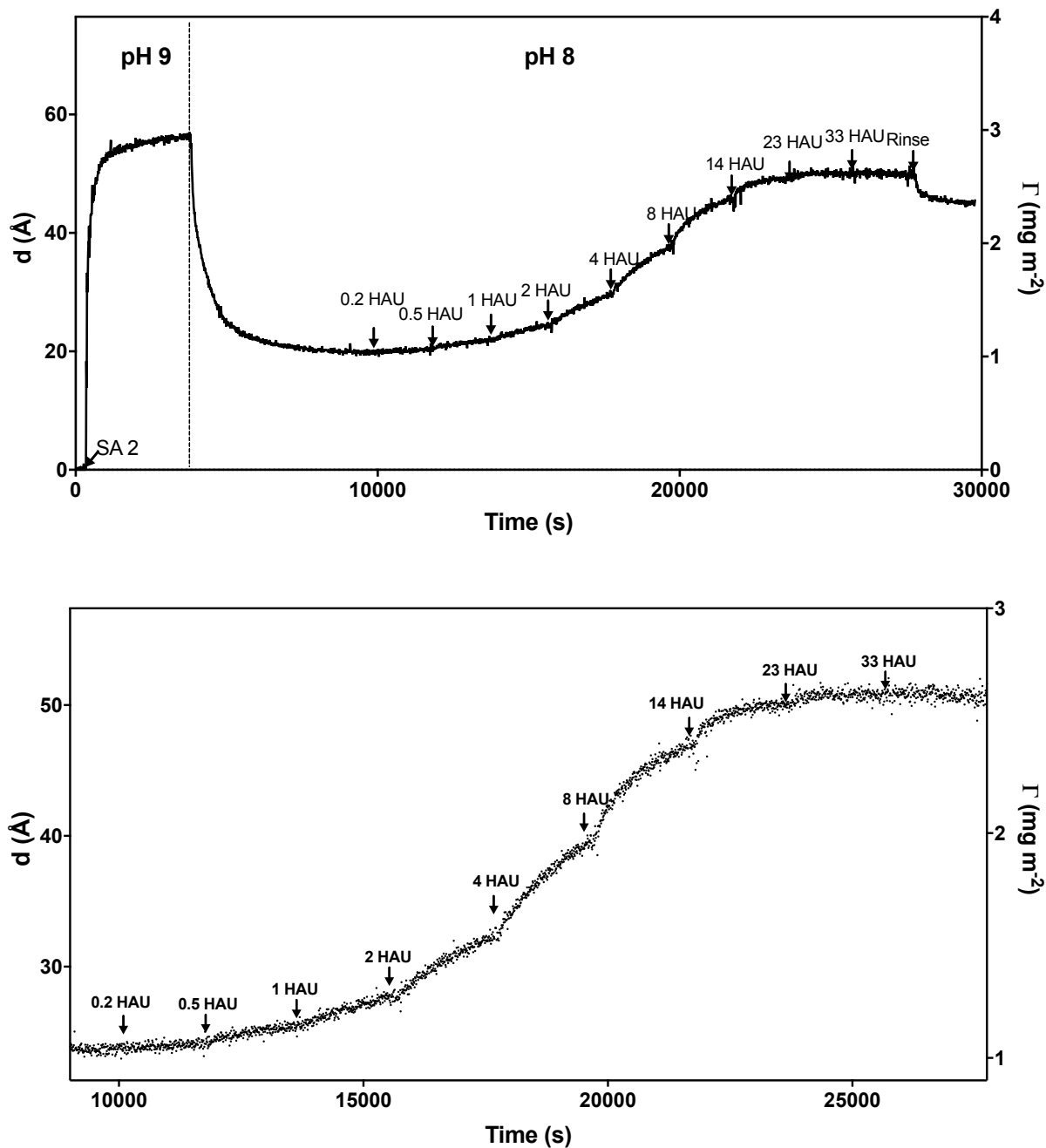


Figure 10. Film thickness, (d), and amount adsorbed, (Γ) estimated by *in situ* ellipsometry, versus time on rSAM-2 modified MHA on gold upon addition of incremental amounts of H5N1 (0.2 to 33 HAUs). Arrows indicate the time of addition of 2 or H5N1 to the system or buffer rinse. The final concentration of H5N1 is given at the top of the arrows. The pH of the system at the given time is indicated at the top of the plot. The pH was changed by continuous rinsing of the system with the buffer of the corresponding pH(top). Expanded plot of the H5N1 addition (bottom).

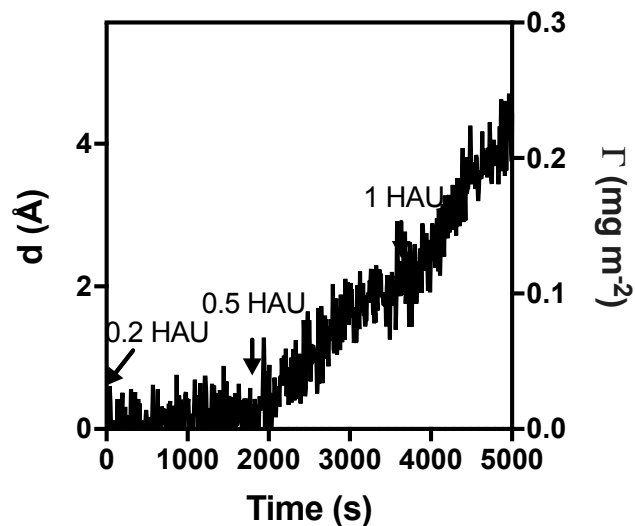


Figure 11. Enlarged section of the plot in Figure 10 showing the change in thickness and amount adsorbed, (Γ), upon addition of 0.2 - 1 HAU of H5N1. Addition of 0.5 HAU consistently resulted in a change of Γ of ca 0.1 mg/m^2 well exceeding three times the standard deviation (SD) of the blank signal (SD=0.017).

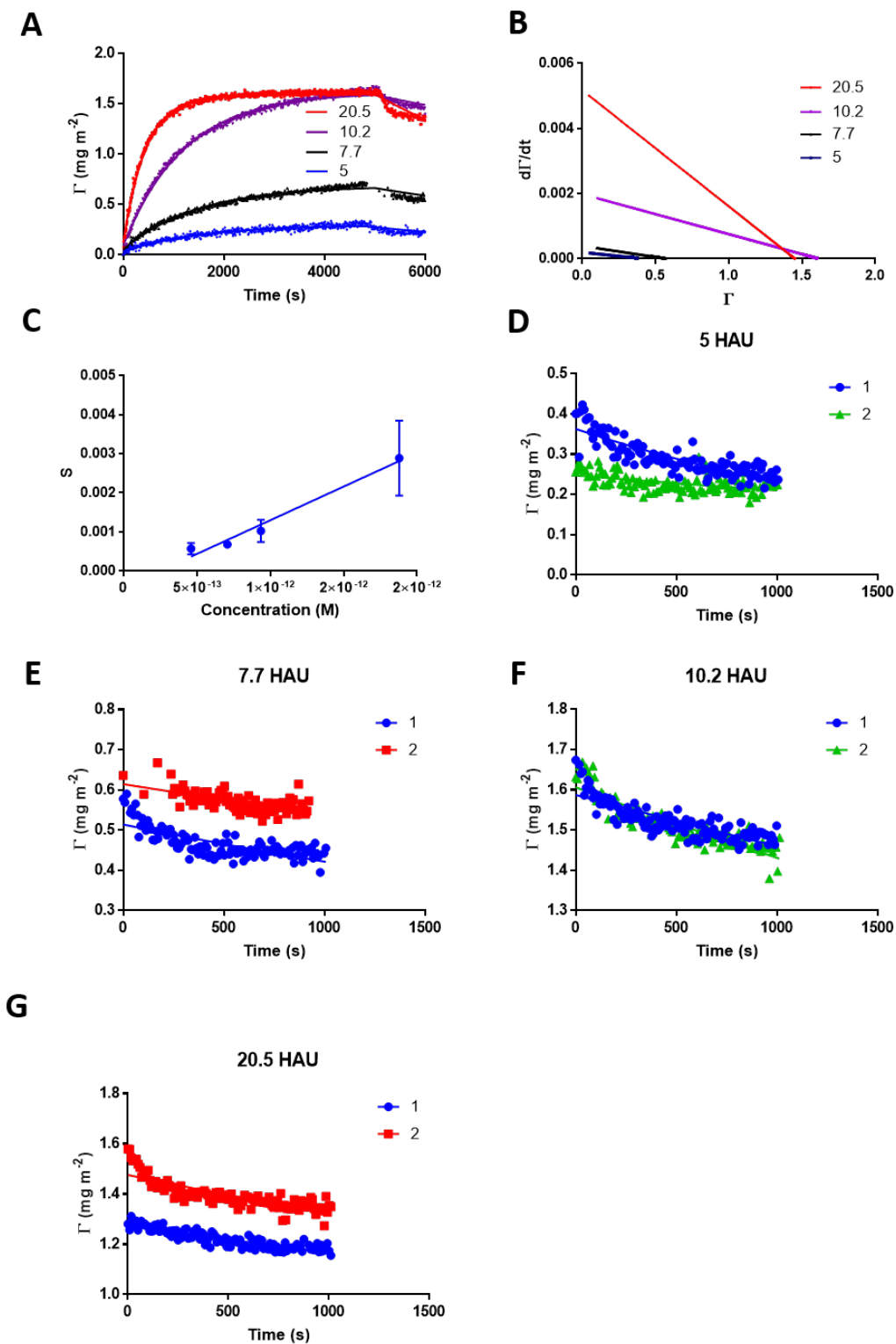


Figure 12. Kinetic interaction analysis used to determine the association and dissociation rate constants k_a and k_d for the interaction between H5N1 and rSAM-2 (see experimental section 1.7). A. Association and dissociation of H5N1 at 4 different concentrations. B. Plot of $d\Gamma/dt$ versus Γ to determine the slope S ($=k_a C - k_d$). C. Linear regression of slope S versus concentration of H5N1 to give the association rate constant, k_a ($1.7 \times 10^9 \text{ M}^{-1} \text{ s}^{-1}$) from the new slope. D-G. Nonlinear curve fitting of the dissociation rate curves in A to Equation 4 to give the average dissociation rate constant, k_d ($2.0 \times 10^{-4} \text{ s}^{-1}$).

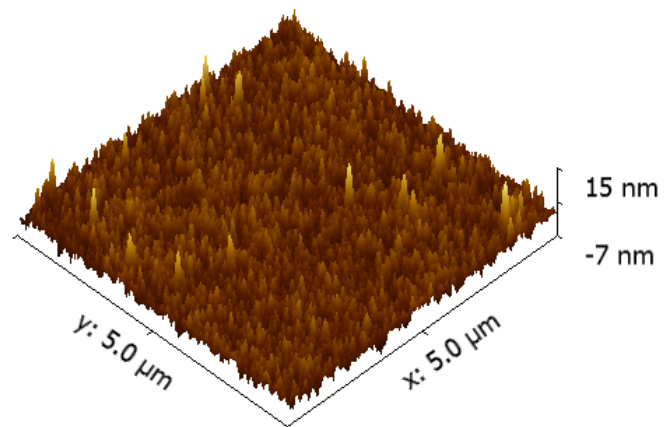


Figure 13. Surface topography of an rSAM-2 on MHA modified gold on glass followed by rinsing with pH 8 HEPES buffer. The surface roughness, R_a was estimated to 1.7 ± 0.1 nm and 2.3 ± 0.3 nm for the surface prior to and after exposure to H5N1 (see Figure 4D) by sampling at random at 3 spots.

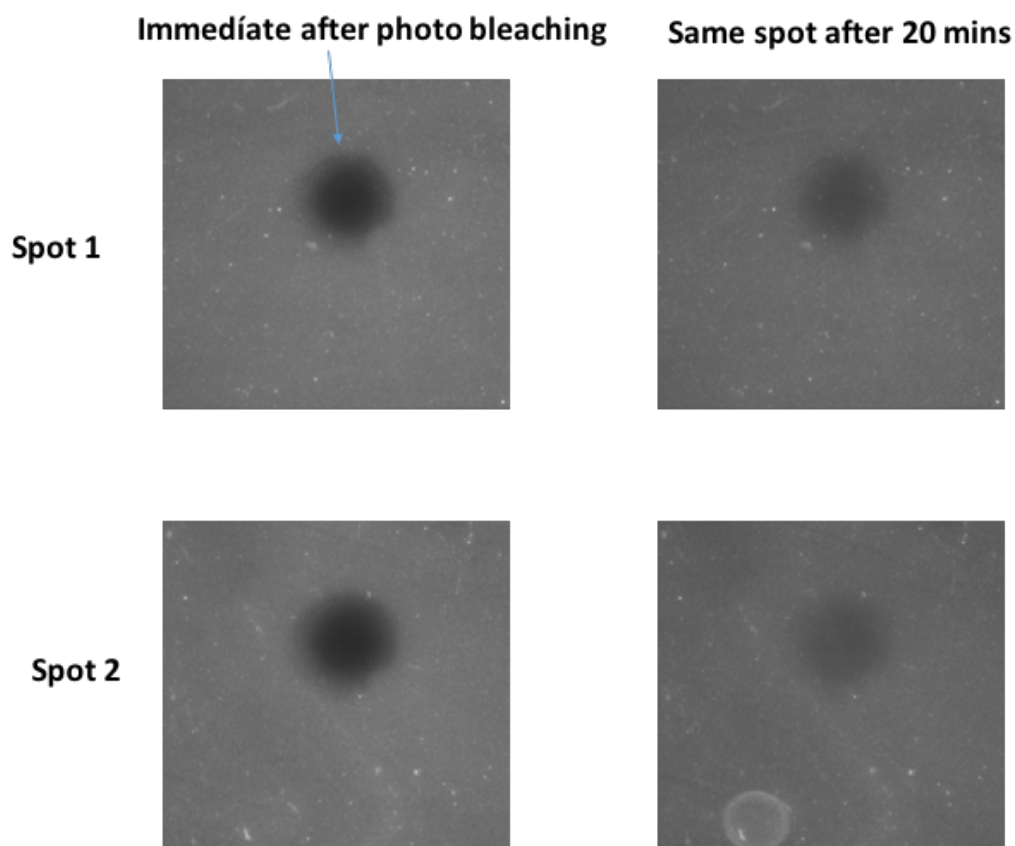
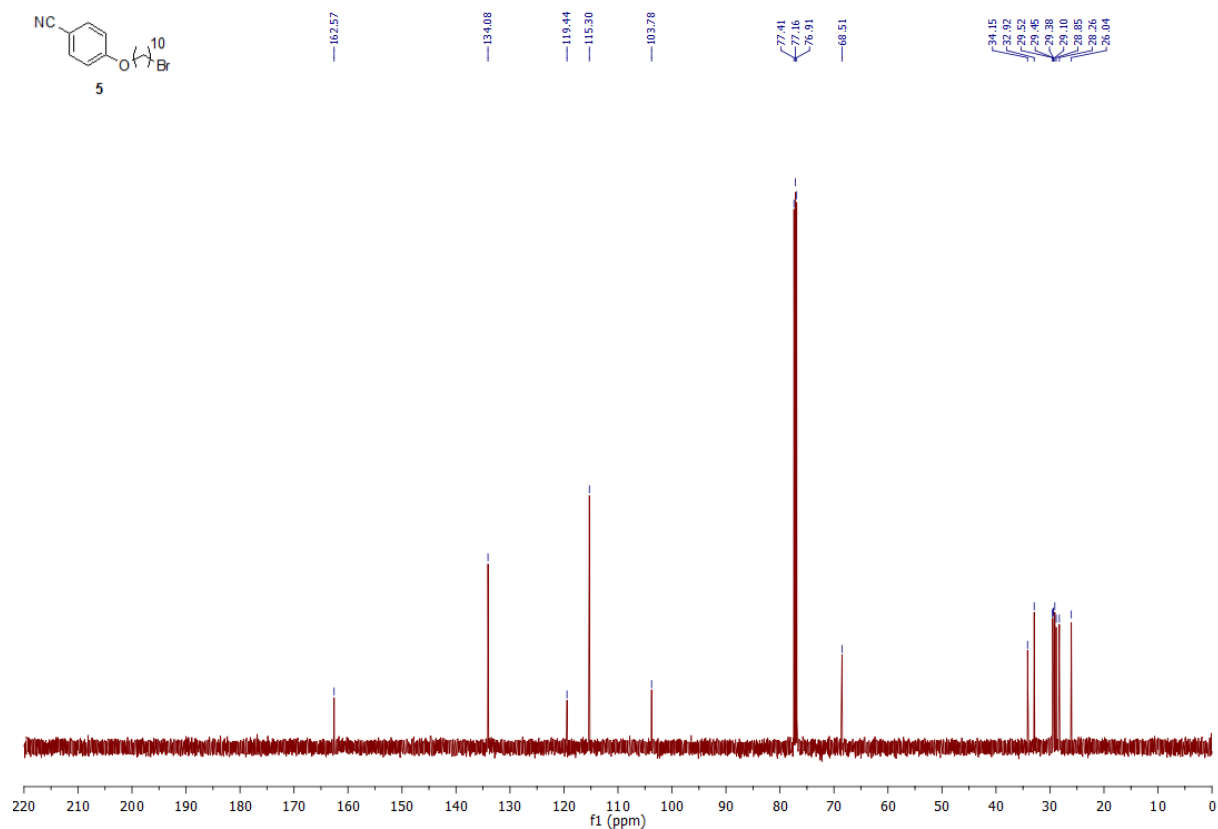
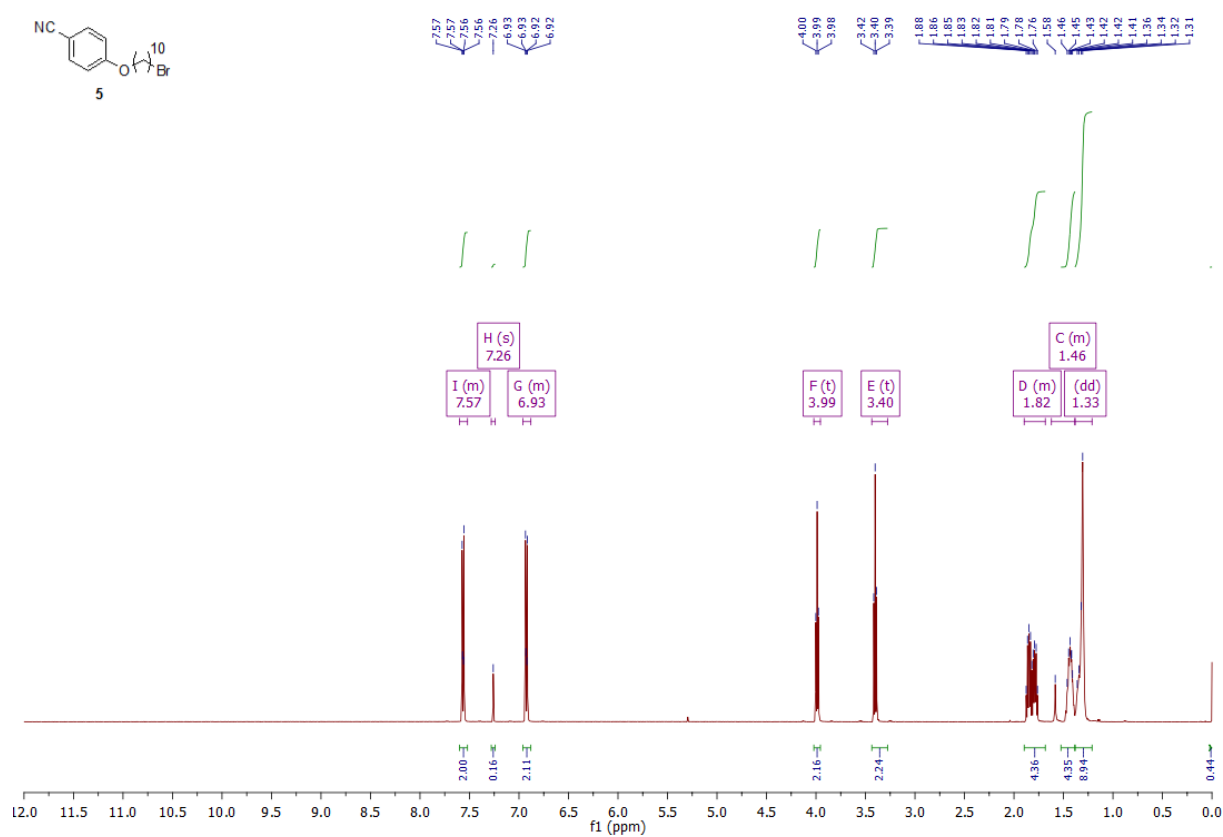
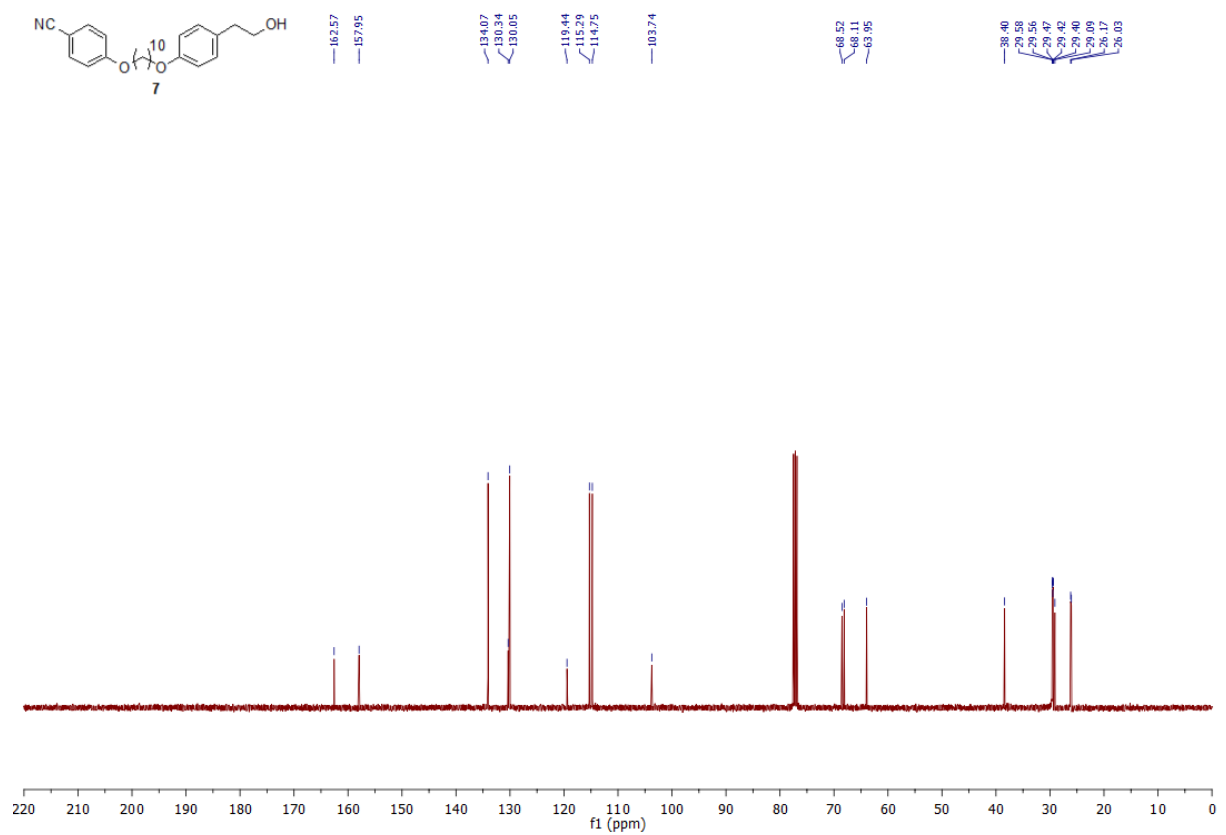
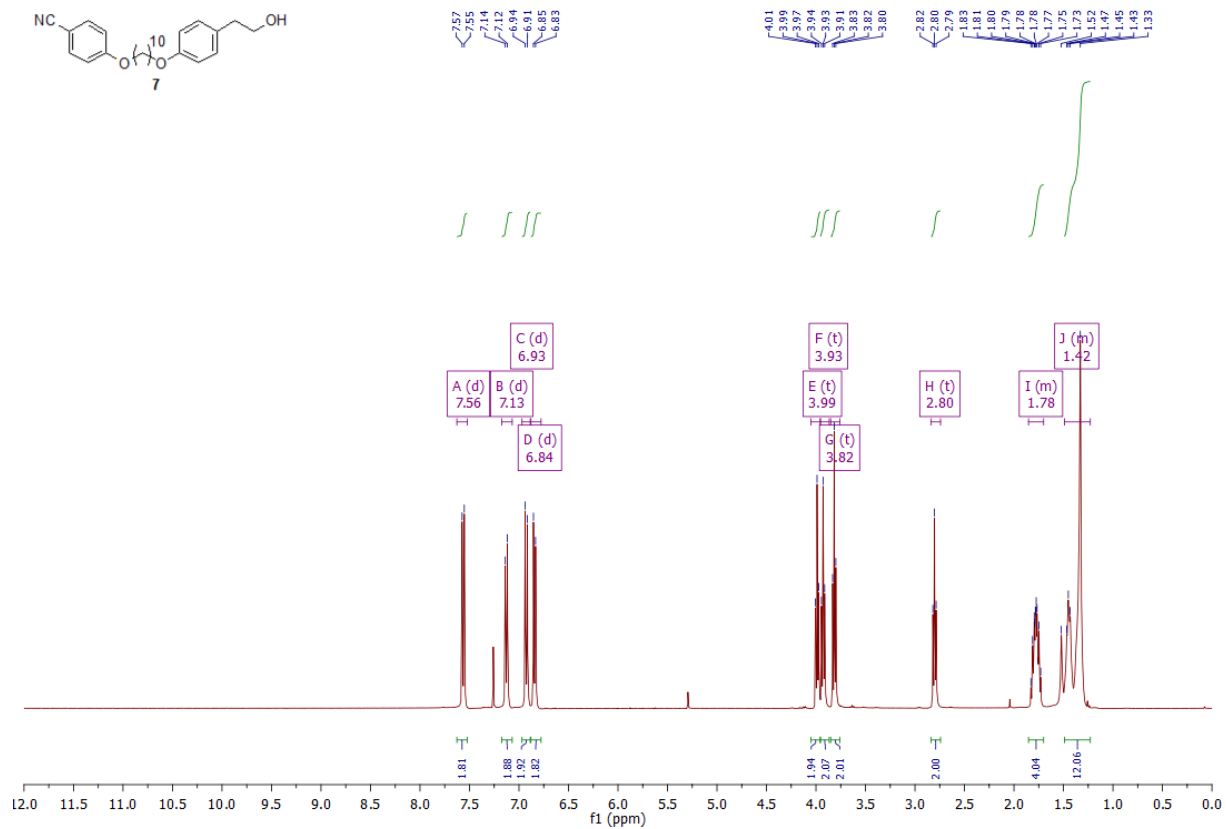
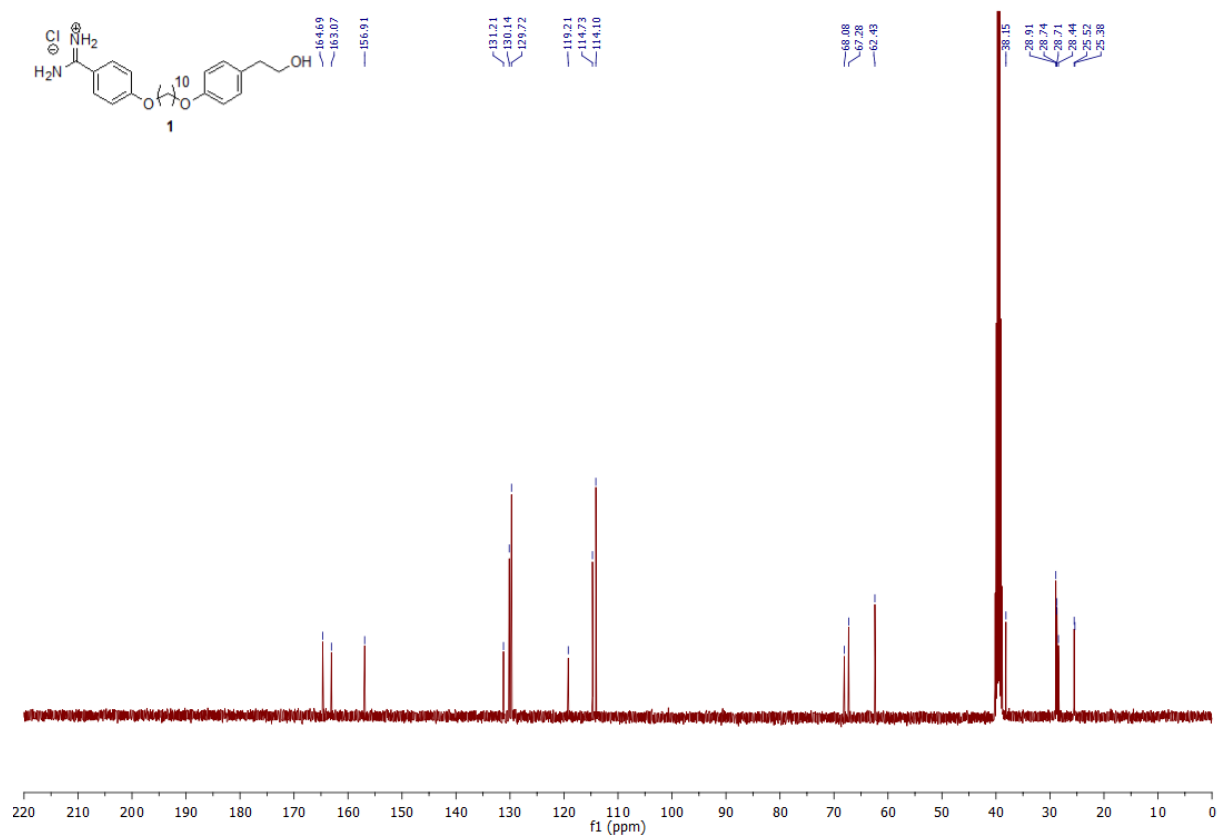
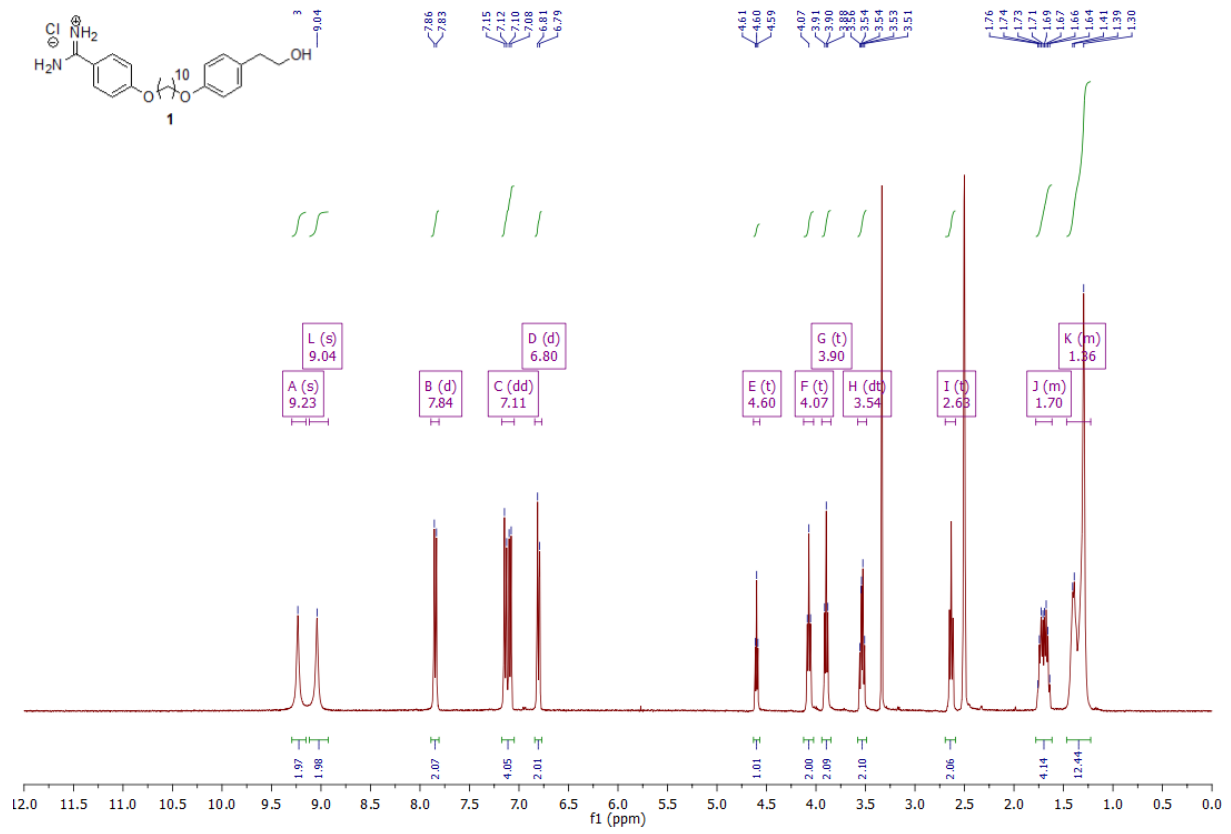


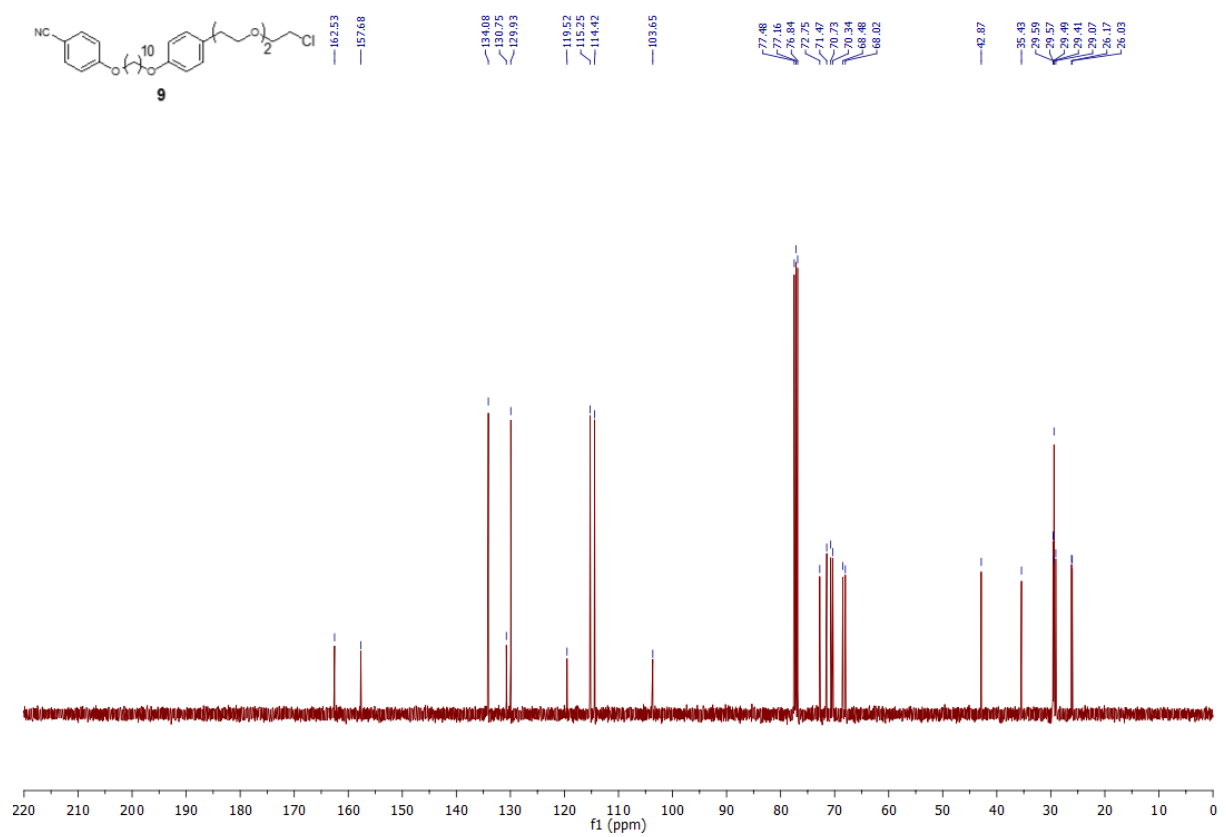
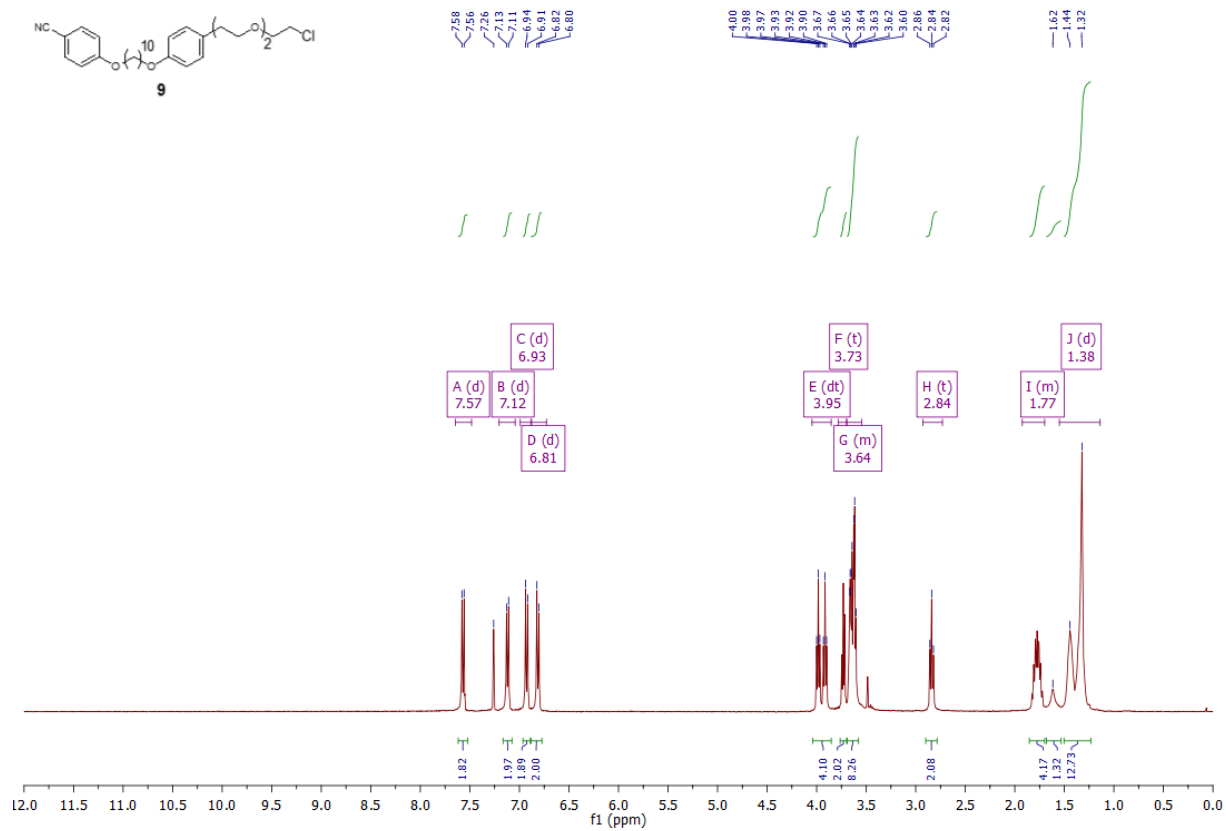
Figure 14. Fluorescence recovery after photobleaching of a carboxylic acid SAM on quartz modified with the EG2 rSAM 15 doped with 1 mol% of fluorescein terminated amphiphile. Bleaching was performed at 488 nm at full power for 30s and images recorded every 30 s for 20 minutes.

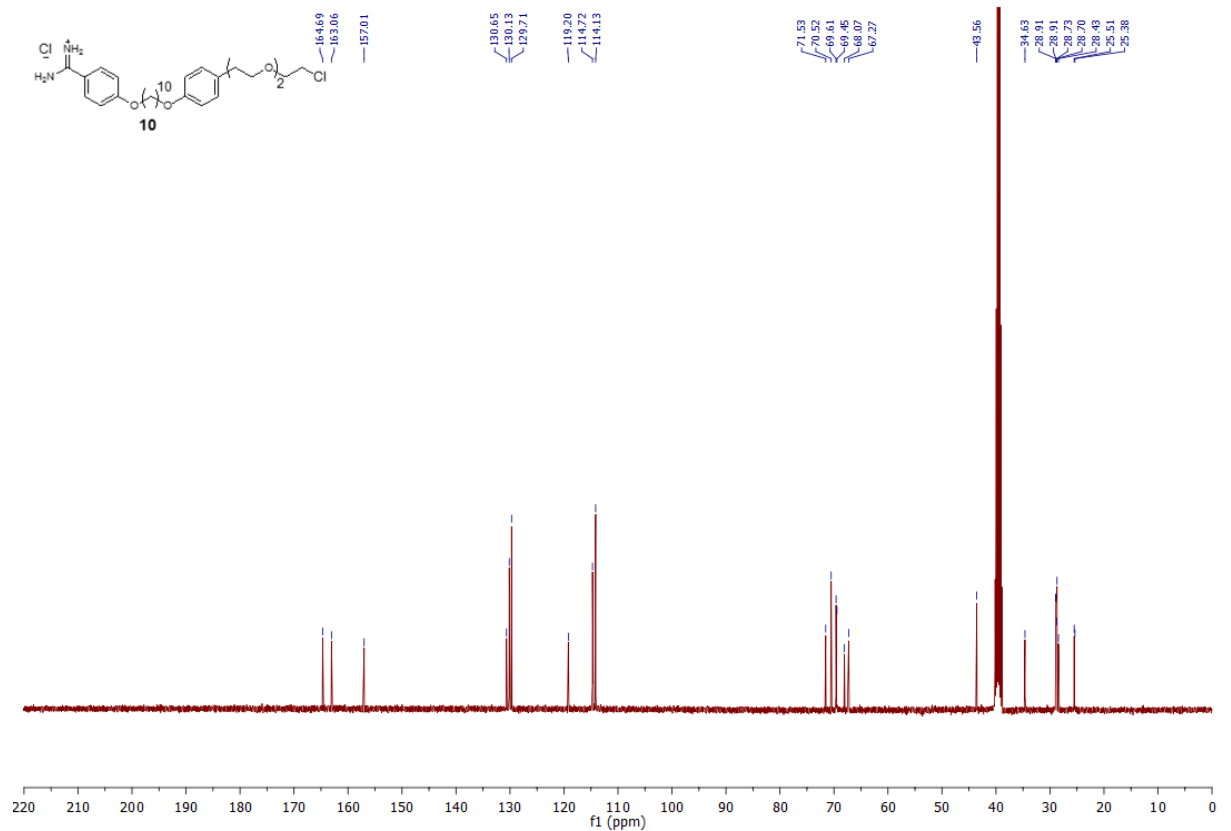
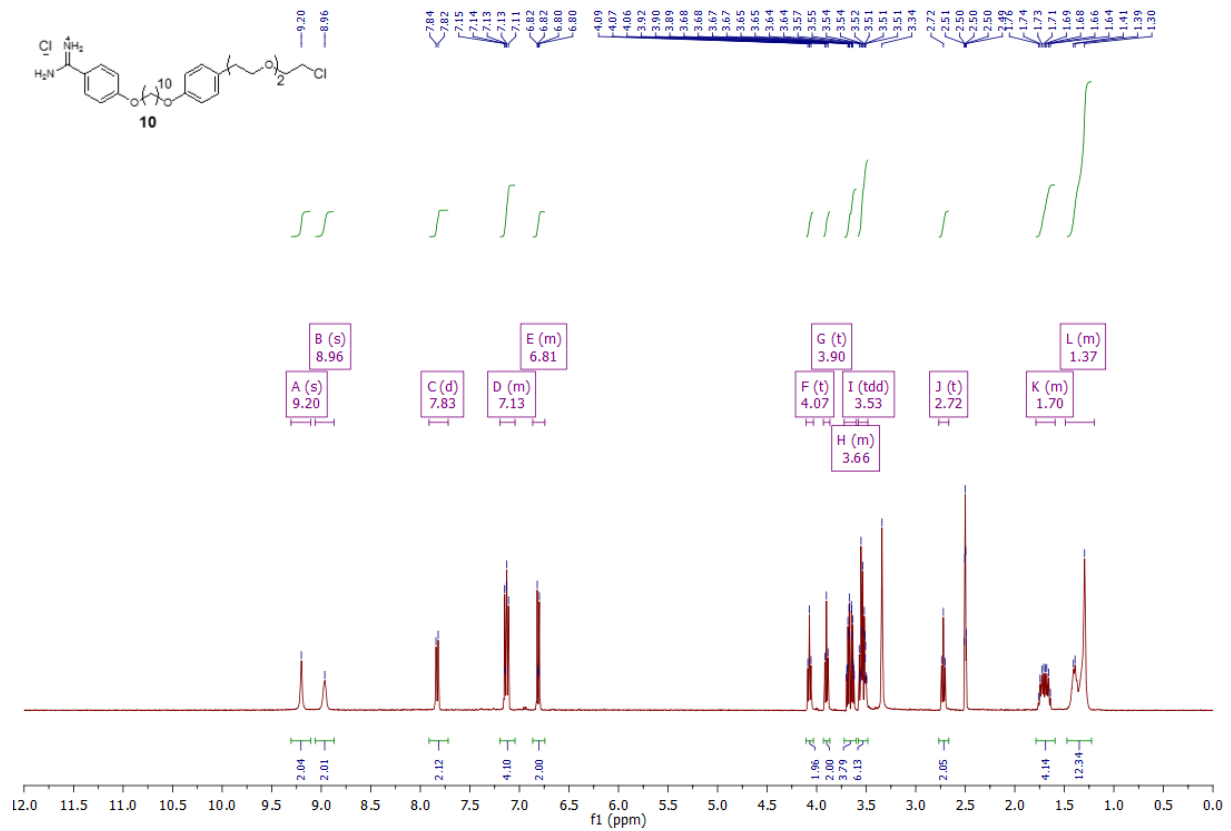
NMR Spectra confirming synthesized compound purity and identity

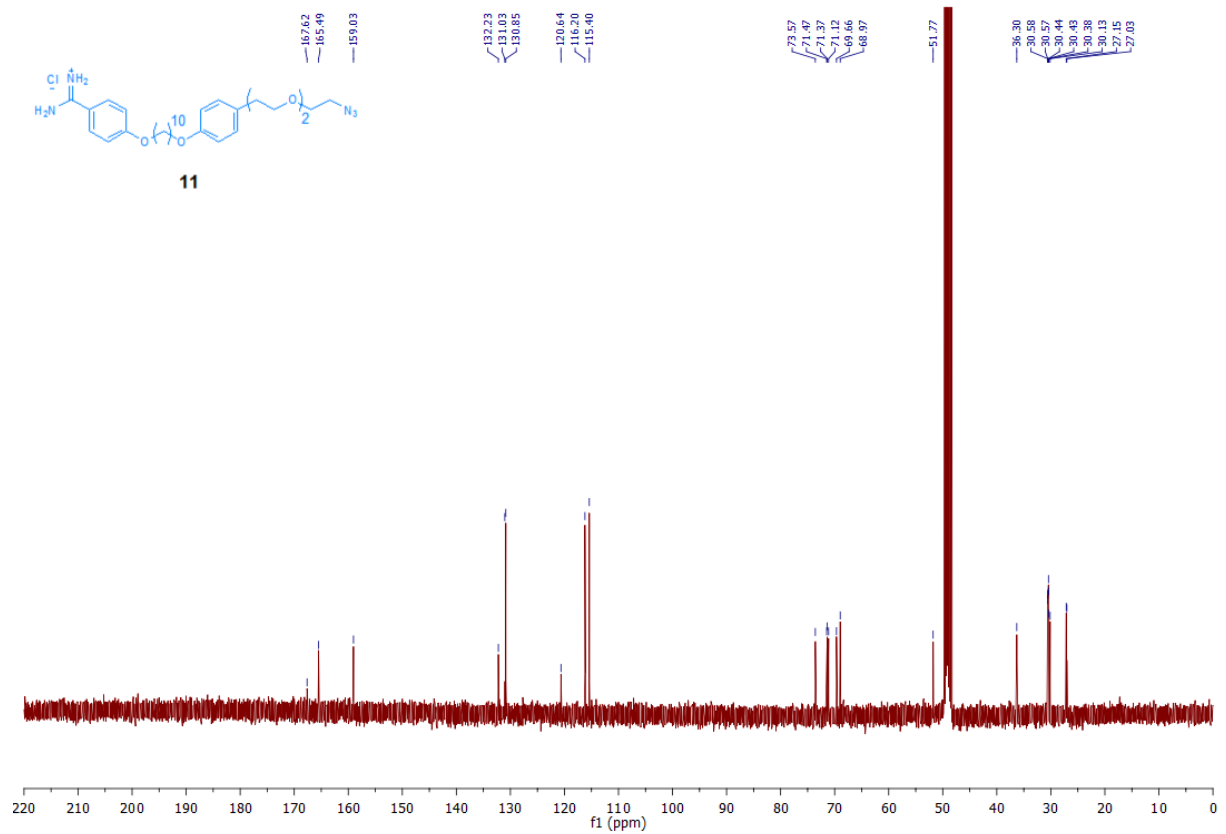
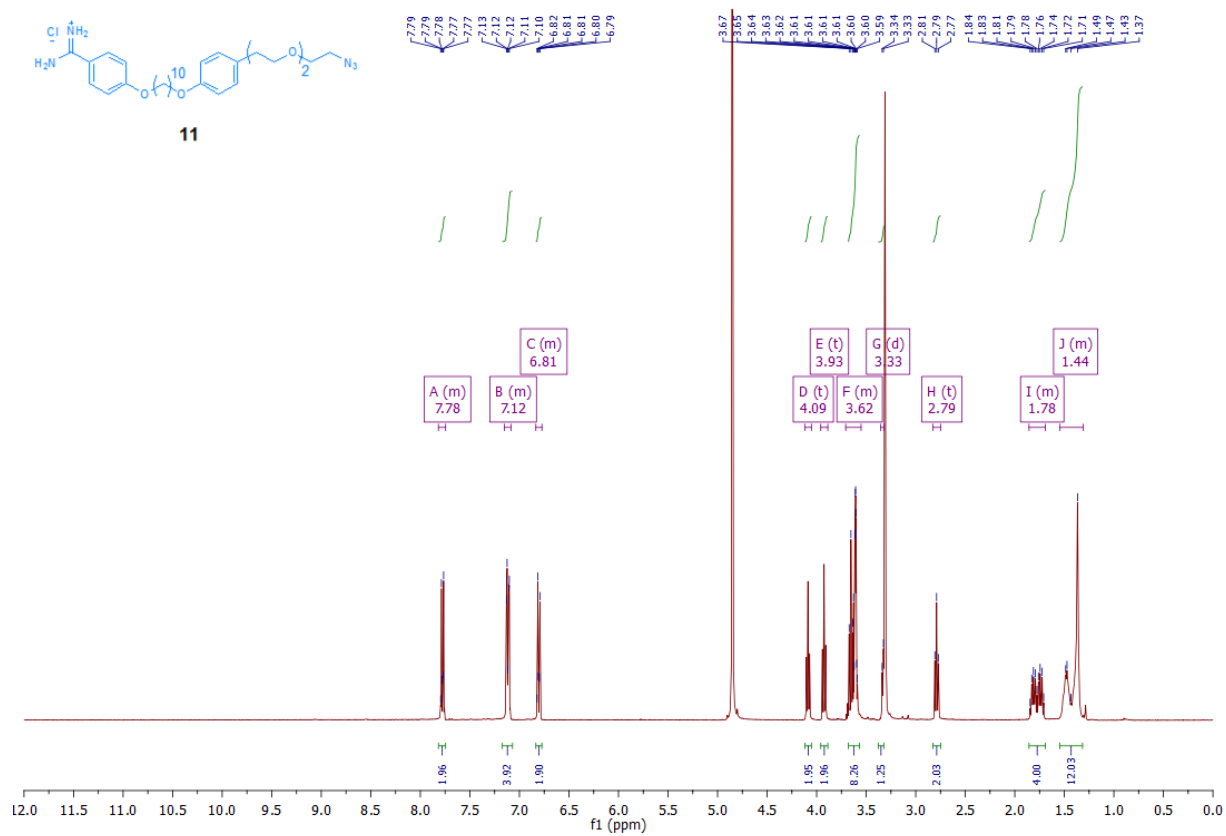


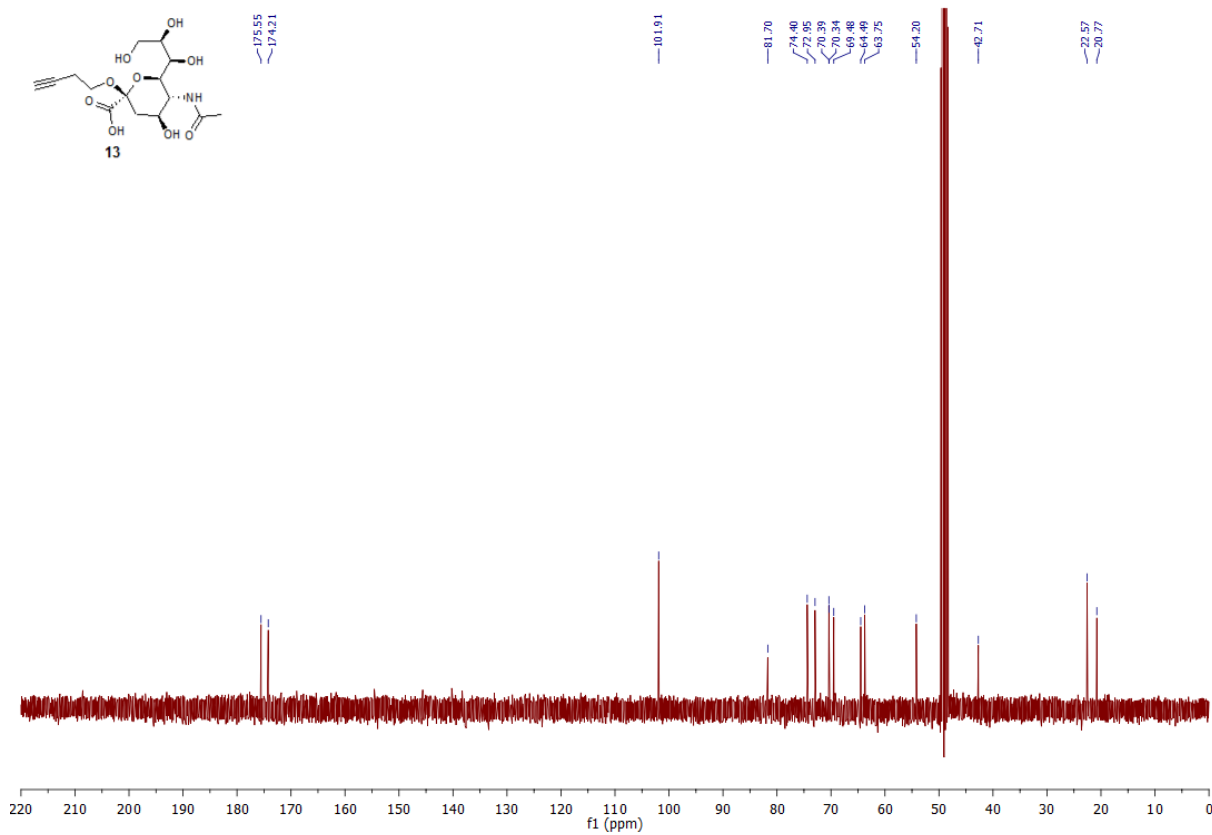
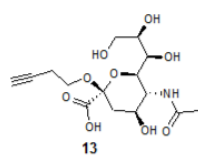
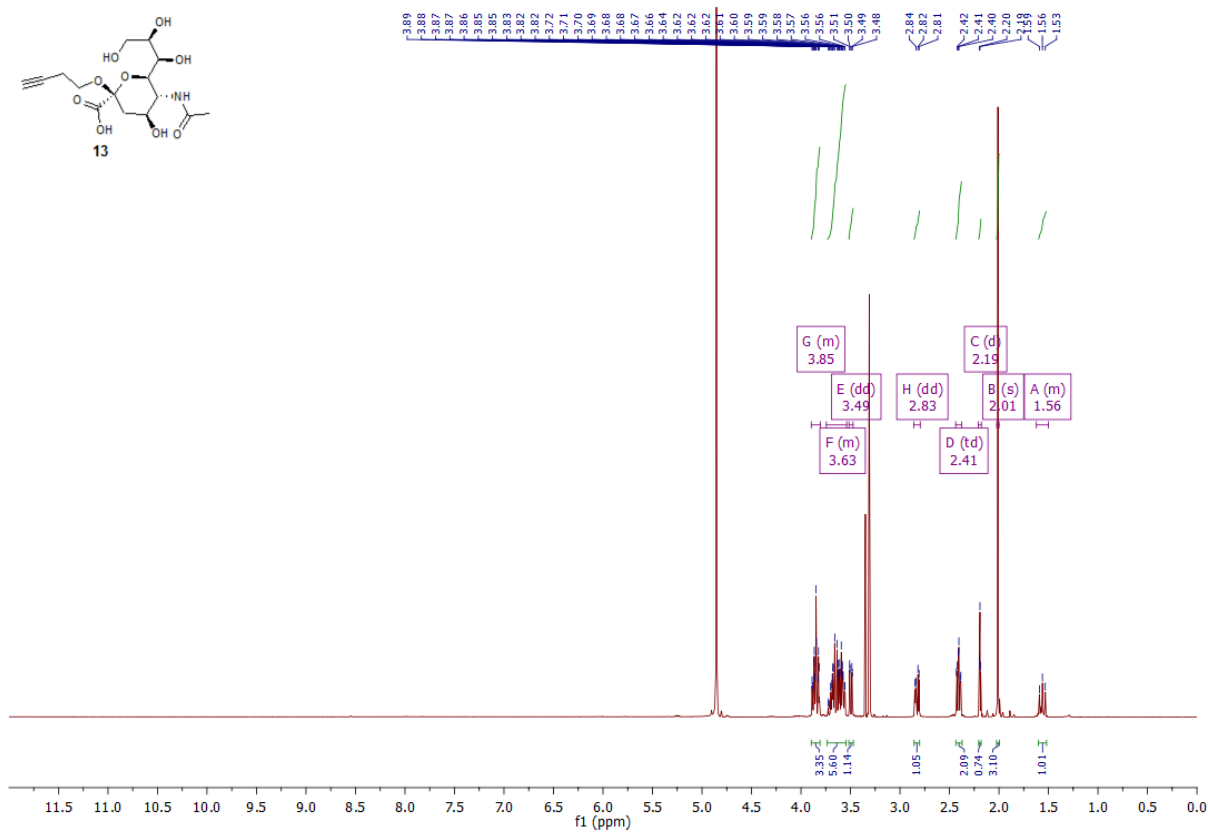
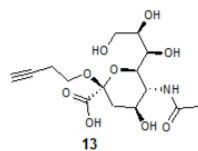


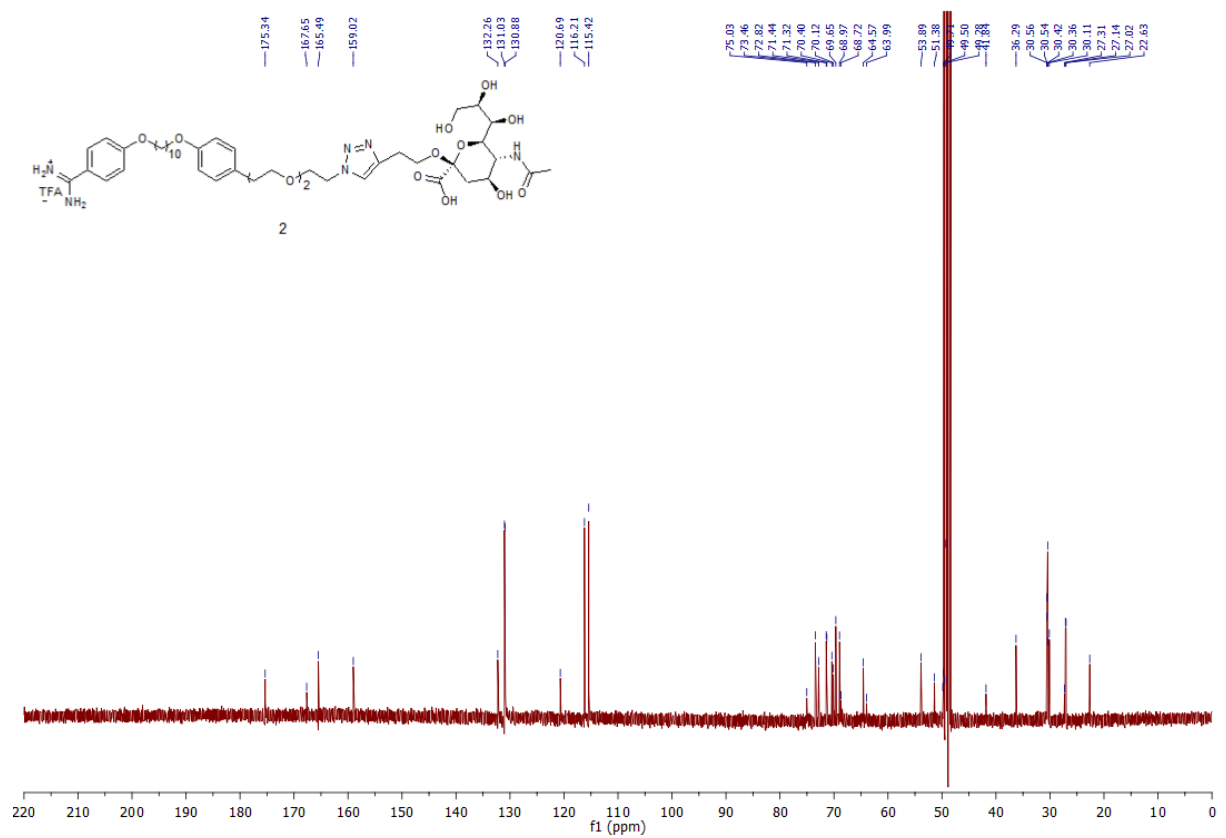
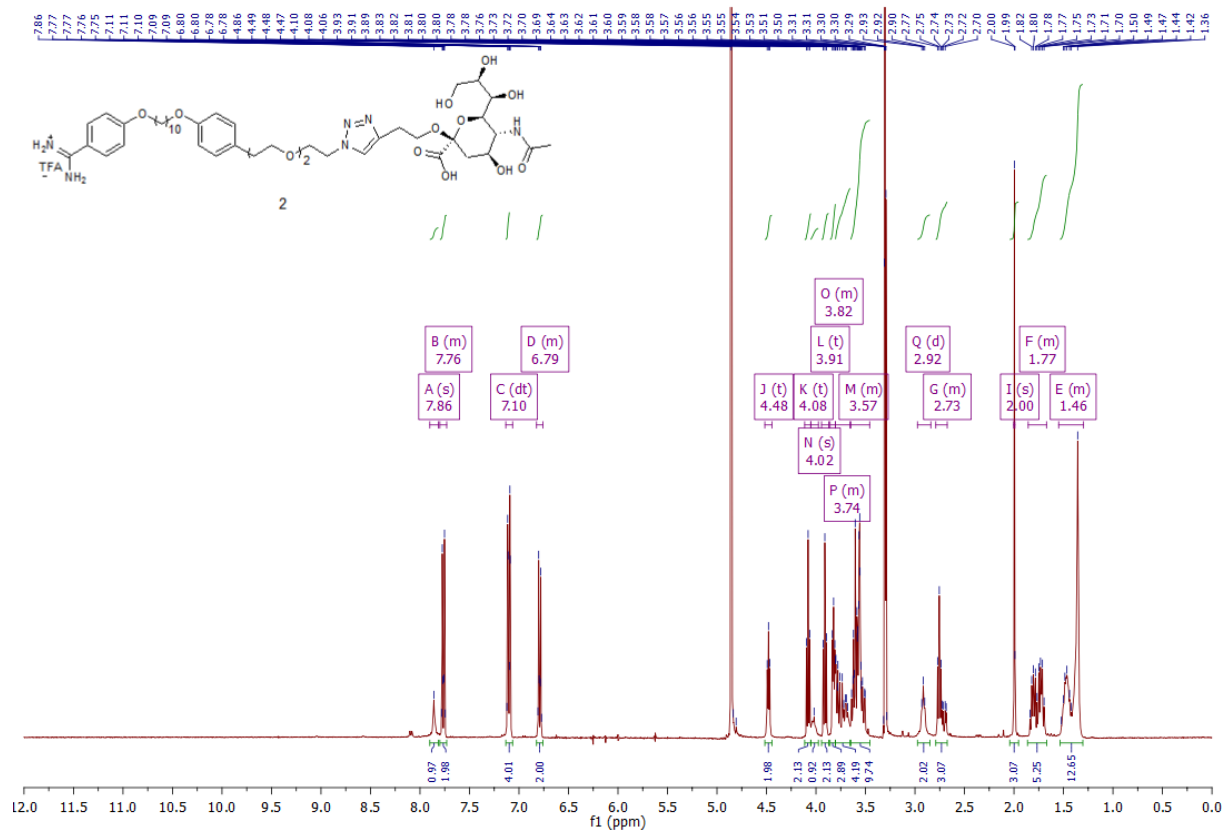






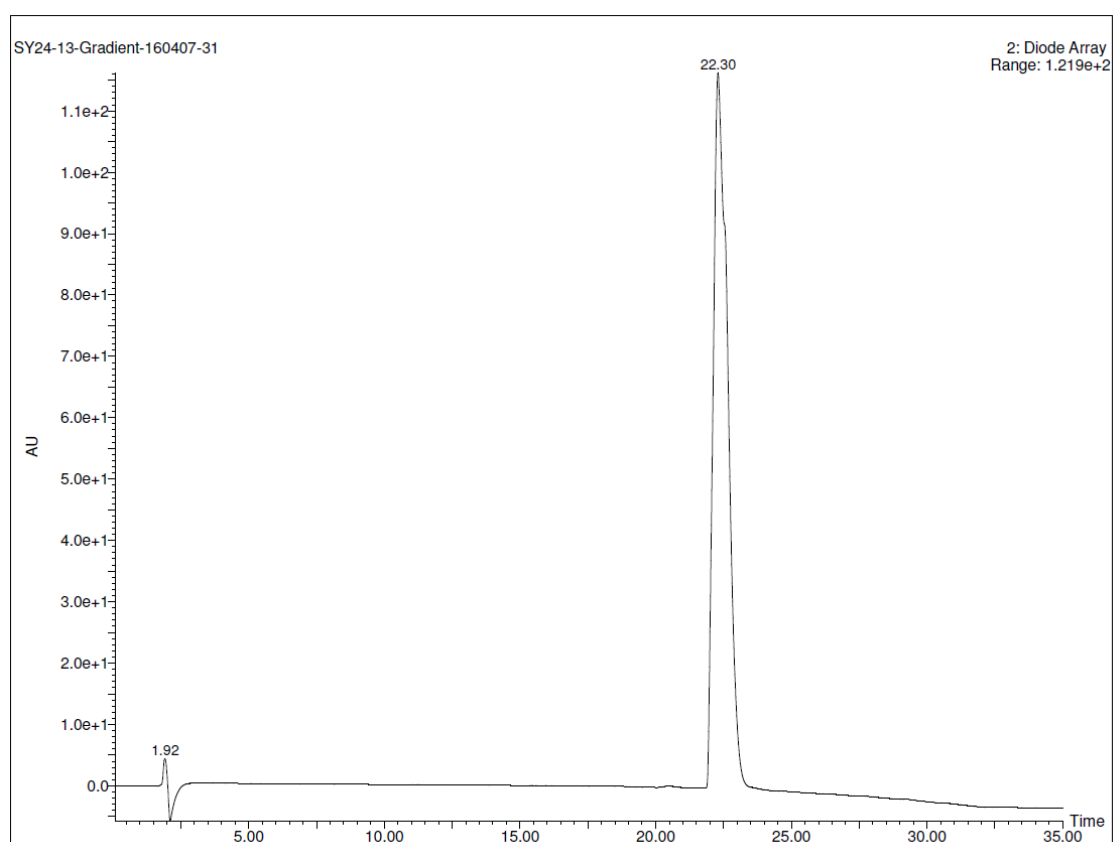






HPLC chromatogram of sialic acid terminated amphiphile 2

C-18 column, mobile phase: 10% - 90 % ACN in water (0.1% TFA) (0-30 mins) 90% ACN in water (0.1% TFA) (30-35 mins)); $k=10.6$.



4 Supplementary Notes

Best-fit values resulting from analysis of the binding data in Figure 4 assuming a Hill cooperative or one site binding model.

	HA on rSAM-2	
One site -- Specific binding with Hill slope		
Best-fit values		
Bmax	0,9161	
h	1,54	
Kd	5,136	
Std. Error		
Bmax	0,02515	
h	0,1702	
Kd	0,4449	
95% CI (asymptotic)		
Bmax	0,8607 to 0,9841	
h	1,194 to 2,01	
Kd	4,197 to 6,416	
Goodness of Fit		
Degrees of Freedom	6	
R square	0,9941	
Absolute Sum of Squares	0,006782	
Sy.x	0,03362	
Number of points	9	
# of X values	9	
# Y values analyzed	0,9161	
	HA on rSAM-1	HA on MHA Ambiguous
One site -- Specific binding		
Best-fit values		
Bmax	21.37	~ 2.726e+014
Kd	459.4	~ 8.425e+015
Std. Error		
Bmax	13.8	~ 1.427e+028
Kd	339.9	~ 4.411e+029
95% CI (asymptotic)		
Bmax	-11.27 to 54.01	(Very wide)
Kd	-344.4 to 1263	(Very wide)
Goodness of Fit		
Degrees of Freedom	7	7
R square	0.9926	0.9695
Absolute Sum of Squares	0.09122	0.06014
Sy.x	0.1142	0.09269
Number of points		
# of X values	9	18
# Y values analyzed	9	9

	HSA on rSAM-2	ConA on rSAM-2
One site -- Specific binding		
Best-fit values		
Bmax	0.0868	1.589
Kd	1.084	60.33
Std. Error		
Bmax	0.006639	0.0823
Kd	0.466	5.951
95% CI (profile likelihood)		
Bmax	0.07109 to 0.1052	1.413 to 1.825
Kd	0.2826 to 3.568	47.82 to 77.76
Goodness of Fit		
Degrees of Freedom	7	7
R square	0.7366	0.9981
Absolute Sum of Squares	0.001217	0.001933
Sy.x	0.01319	0.01662
Number of points		
# of X values	9	9
# Y values analyzed	9	9

	H5N1 on rSAM-2	H5N1 on MHA
One site -- Specific binding with Hill slope		
Best-fit values		
Bmax	1,832	1.082
h	2,15	1.386
Kd	2,341	16.41
Std. Error		
Bmax	0,0174	0.783
h	0,1005	0.7684
Kd	0,05947	19.19
95% CI (asymptotic)		
Bmax	1,79 to 1,875	0.5611 to +infinity
h	1,904 to 2,396	??? to 4.385
Kd	2,195 to 2,486	5.915 to +infinity
Goodness of Fit		
Degrees of Freedom	6	19
R square	0,9991	0.8058
Absolute Sum of Squares	0,004661	0.2656
Sy.x	0,02787	0.1182
Number of points		
# of X values	9	22
# Y values analyzed	9	22

5 Supplementary References

- 1 Tidwell, R. R. *et al.* Analogs of 1,5-bis(4-amidinophenoxy)pentane (pentamidine) in the treatment of experimental *Pneumocystis carinii* pneumonia. *Journal of Medicinal Chemistry* **33**, 1252-1257, doi:10.1021/jm00166a026 (1990).
- 2 Bakunova, S. M. *et al.* Structure–Activity Study of Pentamidine Analogues as Antiprotozoal Agents. *Journal of Medicinal Chemistry* **52**, 2016-2035, doi:10.1021/jm801547t (2009).
- 3 Roy, R. & Laferrière, C. A. Synthesis of protein conjugates and analogues of N-acetylneuraminic acid. *Canadian Journal of Chemistry* **68**, 2045-2054, doi:10.1139/v90-313 (1990).
- 4 Deng, J. *et al.* Construction of Effective Receptor for Recognition of Avian Influenza H5N1 Protein HA1 by Assembly of Monohead Glycolipids on Polydiacetylene Vesicle Surface. *Bioconjugate Chemistry* **20**, 533-537, doi:10.1021/bc800453u (2009).
- 5 Ortega-Muñoz, M., Lopez-Jaramillo, J., Hernandez-Mateo, F. & Santoyo-Gonzalez, F. Synthesis of Glyco-Silicas by Cu(I)-Catalyzed “Click-Chemistry” and their Applications in Affinity Chromatography. *Advanced Synthesis & Catalysis* **348**, 2410-2420, doi:10.1002/adsc.200600254 (2006).
- 6 Deng, L., Norberg, O., Uppalapati, S., Yan, M. & Ramstrom, O. Stereoselective synthesis of light-activatable perfluorophenylazide-conjugated carbohydrates for glycoarray fabrication and evaluation of structural effects on protein binding by SPR imaging. *Organic & Biomolecular Chemistry* **9**, 3188-3198, doi:10.1039/C1OB05040K (2011).
- 7 Lin, S., Shih-Yuan Lee, A., Lin, C.-C. & Lee, C.-K. Determination of Binding Constant and Stoichiometry for Antibody-Antigen Interaction with Surface Plasmon Resonance. *Current Proteomics* **3**, 271-282, doi:10.2174/157016406780655586 (2006).
- 8 David Nečas, Petr Klapetek, Gwyddion: an open-source software for SPM data analysis, *Cent. Eur. J. Phys.* 10(1) (2012) 181-188